The Main Sequence of Quasars

and its potential for Cosmology

Paola Marziani[1]

on behalf of "the extreme team"

A. del Olmo[2], D. Dultzin[3], A. Negrete[3], M.L. Martínez-Aldama[4], M. D'Onofrio[5], E. Bon[6], N. Bon[6], S. Panda[7], M. Śniegowka[7], B. Czerny[7], A. Deconto Machado[2], T. Buendia[3], M. Berton[8], E.Järvelä[9], A. de Diego[3], J. Perea[2] et al.

[1]National Institute for Astrophysics, INAF - Osservatorio Astronomico di Padova, Padova, Italy
[2]Instituto de Astrofísica de Andalucía (CSIC), Granada, Spain
[3]Instituto de Astronomía, UNAM, México, D.F., Mexico
[4]Dipartamento de Astronomía, Universidad de Chile, Santiago, Chile
[5]INAF - Osservatorio di Astrofisica e Scienze dello Spazio, Bologna, Italy
[5]Dipartimento di Fisica ed Astronomia "Galileo Galilei", U. di Padova, Padova, Italy
[6]Belgrade Astronomical Observatory, Belgrade, Serbia
[7]Center for Theoretical Physics, Polish Academic of Sciences, Warsaw, Poland
[8]European Southern Observatory (ESO), Santiago, Chile
[9]BEurpopean Spece Agency (ESA), Villanueva de la Cañada, Spain

May 18, 2022 —

Introduction

A main sequence (MS) for type-1 (unobscured) active galactic nuclei

Data-oriented interpretation of the main trends along the MS: two distinct populations Population A and B

Extreme Population A: super-Eddington accretors?

Cosmological applications?

Introduction

Introduction

AGN are understood as accreting supermassive black holes, axially symmetric

Unification schemes: obscured and unobscured (type-2 and type-1), accreting black holes seen at different viewing angles

Unification schemes do not make any prediction for type 1 AGN. <u>Orientation</u> complicates estimates of Eddington ratio, M_{BH}, accretion rate, radiative efficiency

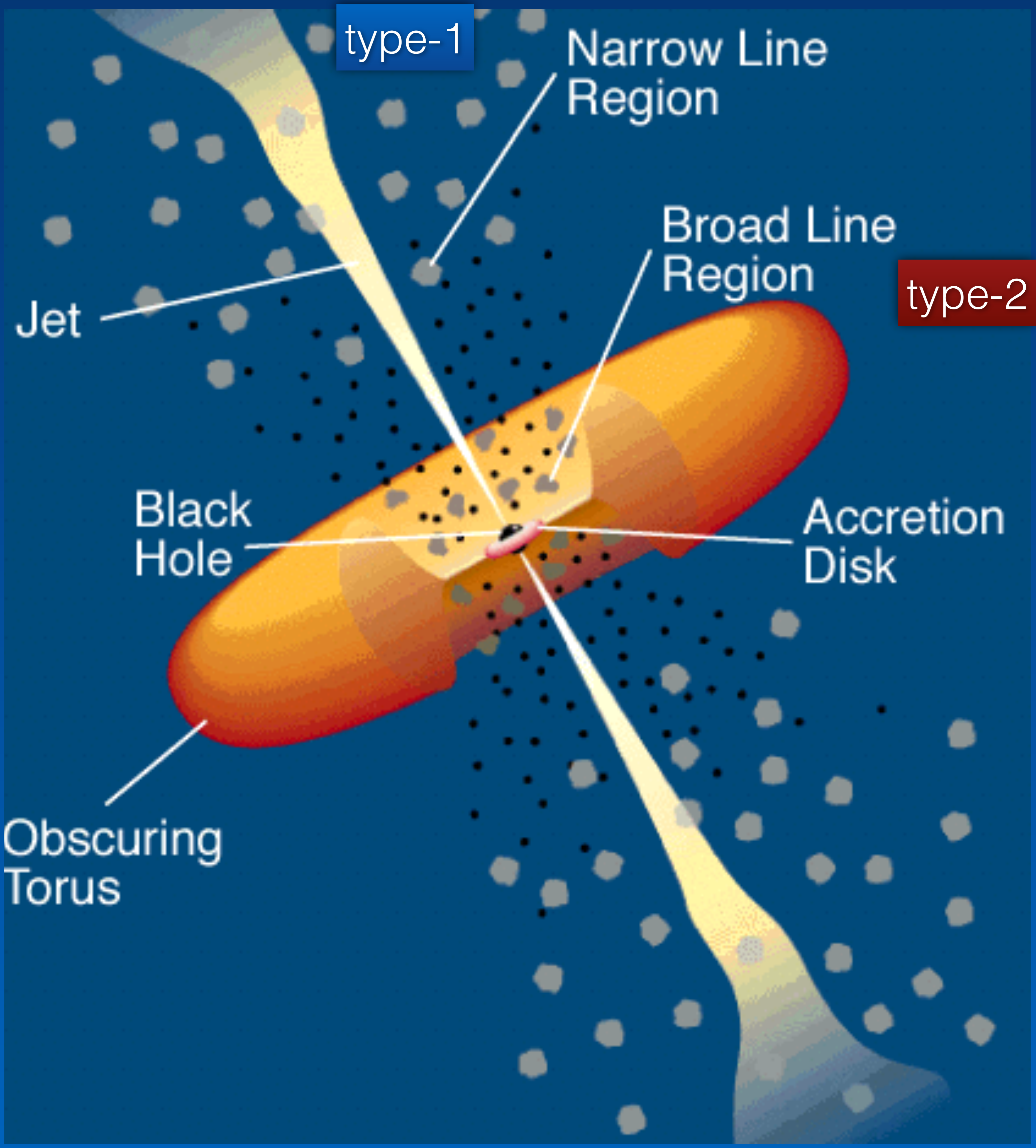

Urry and Padovani 1995

Introduction — The average quasar (type-1) spectrum

Broad and narrow optical and UV lines emitted by ionic species over a wide range of IPs.

	Broad	Narrow
High Ionization (HILs; IP > 30eV)	**CIVλ1549**, HeII	[OIII]λλ4959,5007, HeII,NeIII
Low Ionization (LILs; IP < 15 eV)	Balmer (**Hβ**), FeII, MgIIλ2800, CaII IR Triplet)	Balmer, [OI]λ6300, [SII]λλ6716,6731

CIVλ1549 and Hβ assumed as representative of HILs and LILs

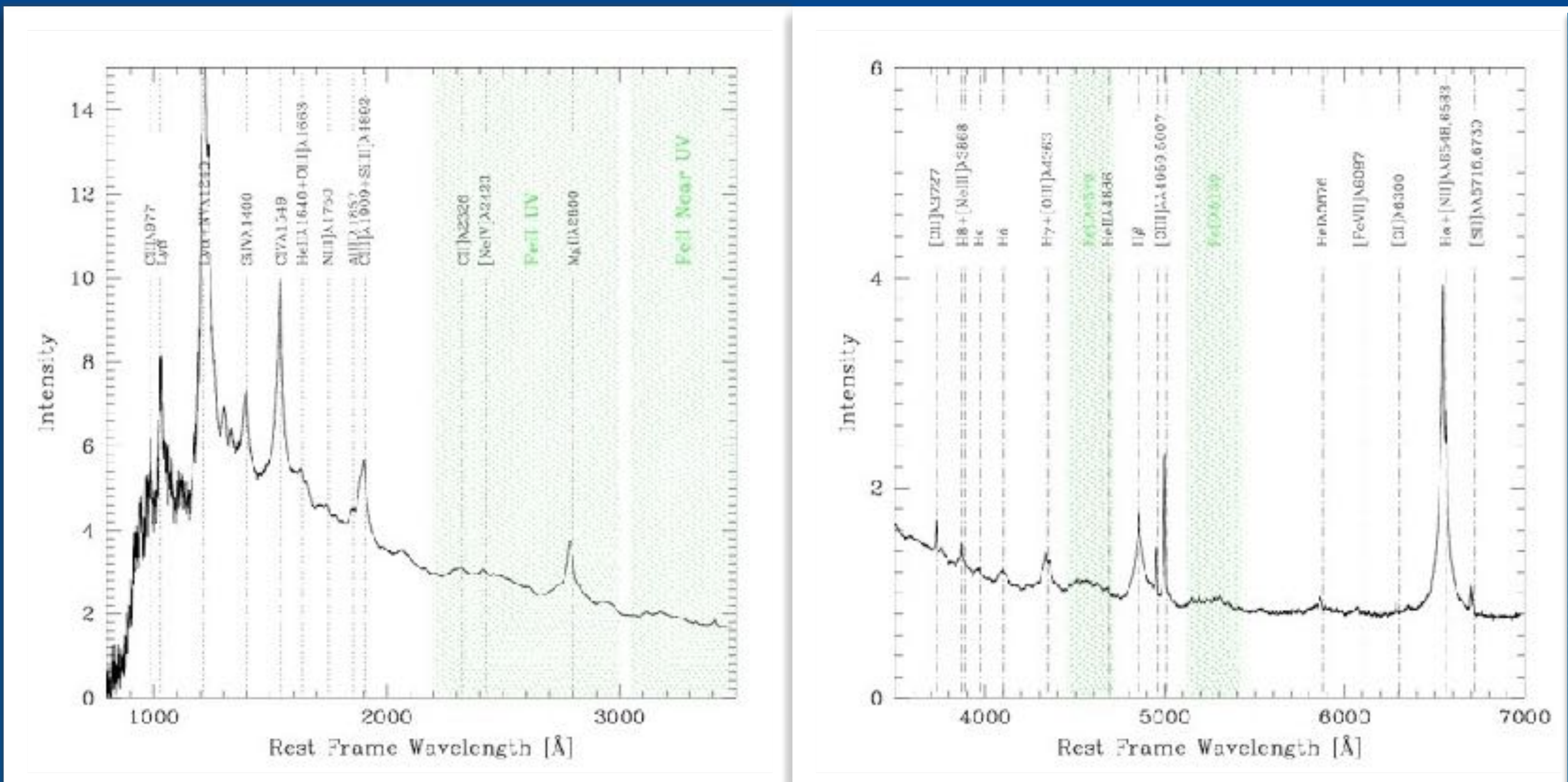

Internal line shifts and intensity ratios between HILs and LILs provide dynamical and physical diagnostics

The composite quasar spectrum from the Sloan DSS (Van den Berk et al. 2001; from Marziani et al. 2006)

The Quasar Main Sequence

The Main Sequence — Organizing quasar diversity

Quasar spectra show systematic differences in line profiles, shifts, intensities ➜ different dynamical and physical conditions of the broad line emitting region (BLR)

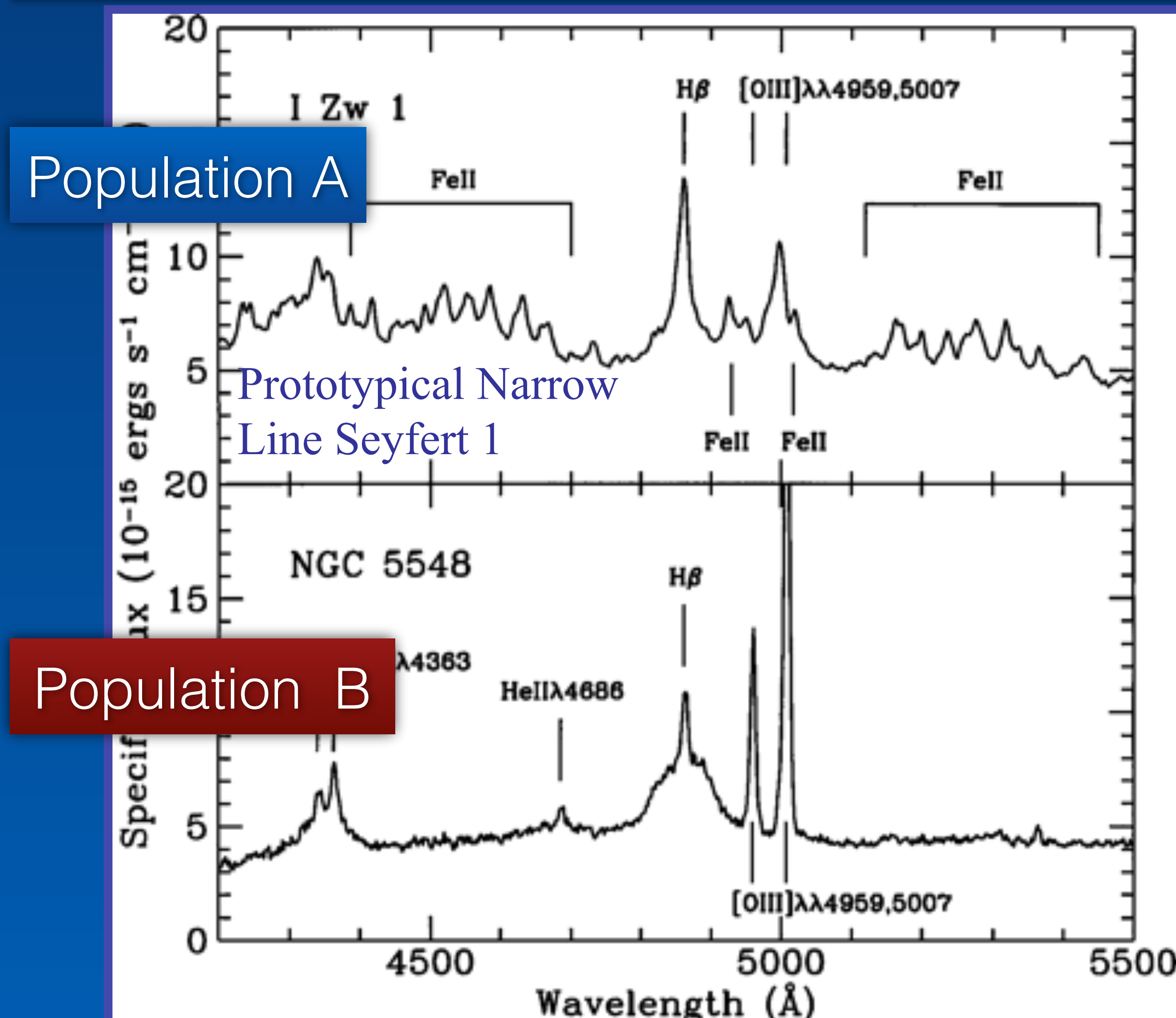

Hβ spectral range

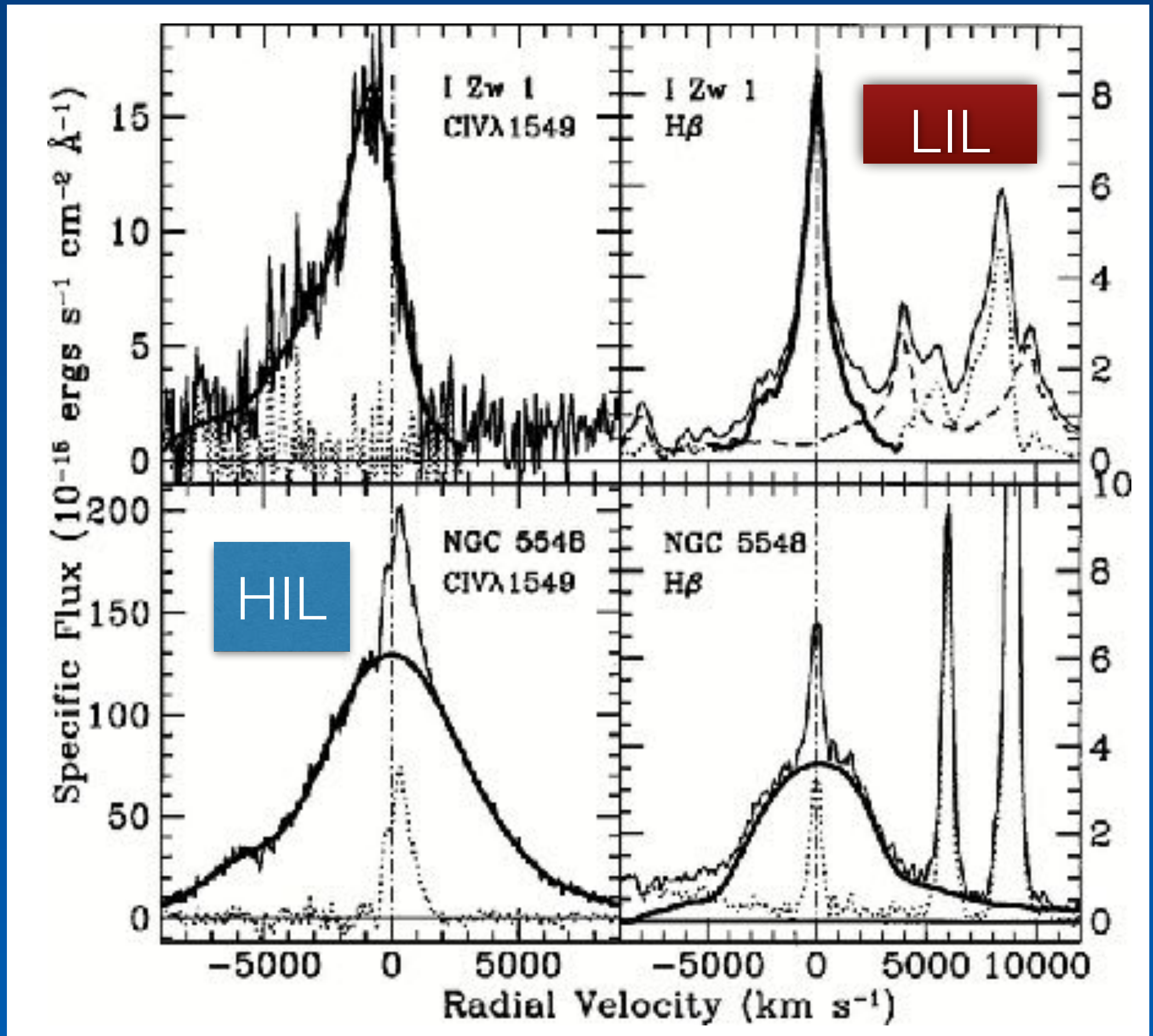

CIV and Hβ (high and low ionization lines)

Population A with (FWHM Hβ<4000 km/s) and Population B

Sulentic et al. 2000

A main sequence for quasars: organizing quasar diversity

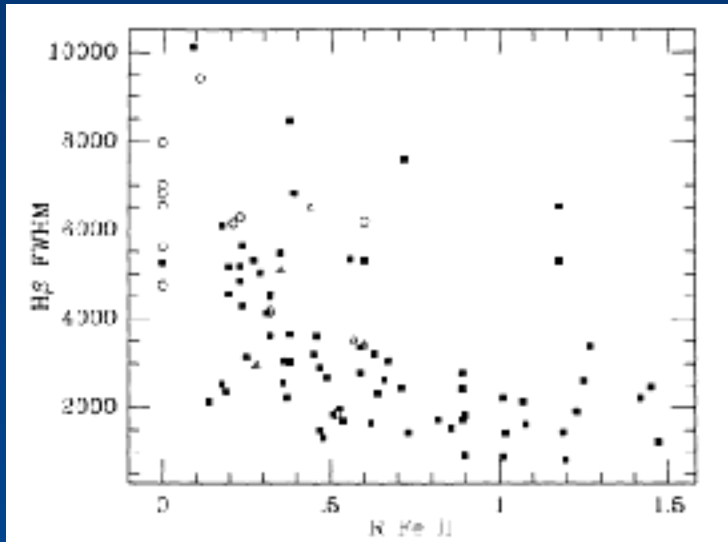

FIG. 5.—FWHM of the Hβ line plotted against R Fe II, the ratio of the equivalent width of the Fe II complex between λ4434 and λ4684 to that of Hβ.

Eigenvector 1 (E1): originally defined by a Principal Component Analysis of parameters measured on the optical spectra of ~80 PG quasars

Boroson & Green 1992; c.f. Gaskell 1985

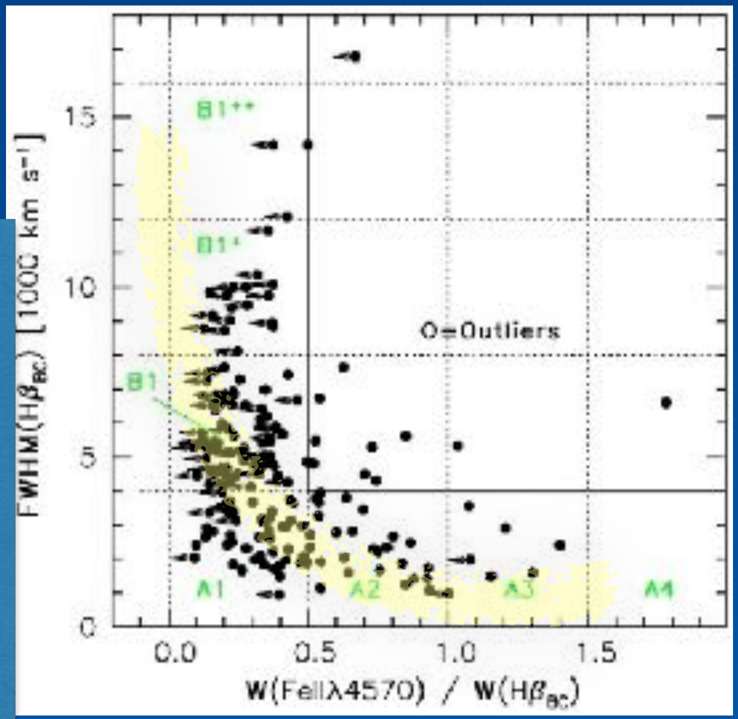

Sulentic et al. 2000 [ARA&A], 2002; n ~ 200

E1 main sequence (MS) first associated with an anti-correlation between strength of FeIIλ4570 and width of Hβ (or the peak intensity of [OIII] 4959,5007)

Since 1992, the E1 MS has been found in increasingly larger samples

Zamfir et al. 2010, n ~ 500

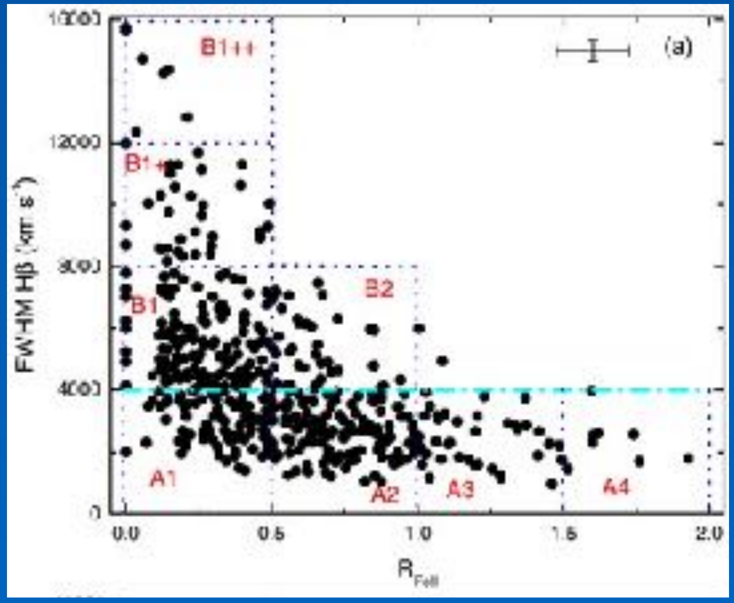

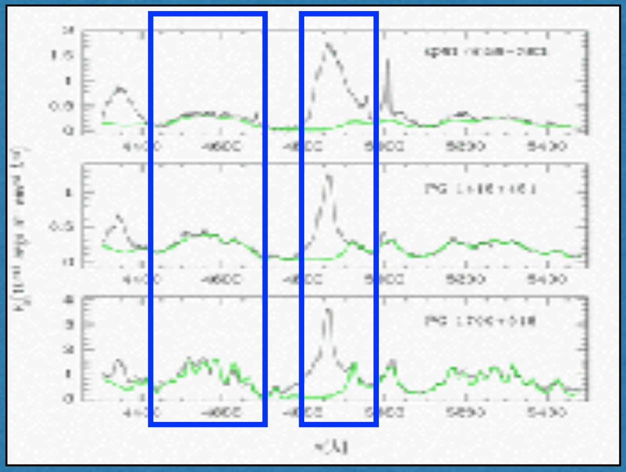

$$R_{\rm FeII} = \frac{I({\rm FeII}\lambda4570)}{I(H\beta)} \approx \frac{W({\rm FeII}\lambda4570)}{W(H\beta)}$$

FeII emission is self-similar but intensity with respect to Hβ changes from object to object

FeII emission from UV to the IR can dominate the thermal balance of the low-ionization BLR

Marinello et al. 2018

FWHM(Hβ): related to the velocity field in the low-ionization BLR (predominantly virialized)

Peterson & Wandel 2000; recent reverberation studies

The main sequence

Quasar spectra diverse line profiles, R_{FeII}, line shifts, line intensities can be organized along the MS

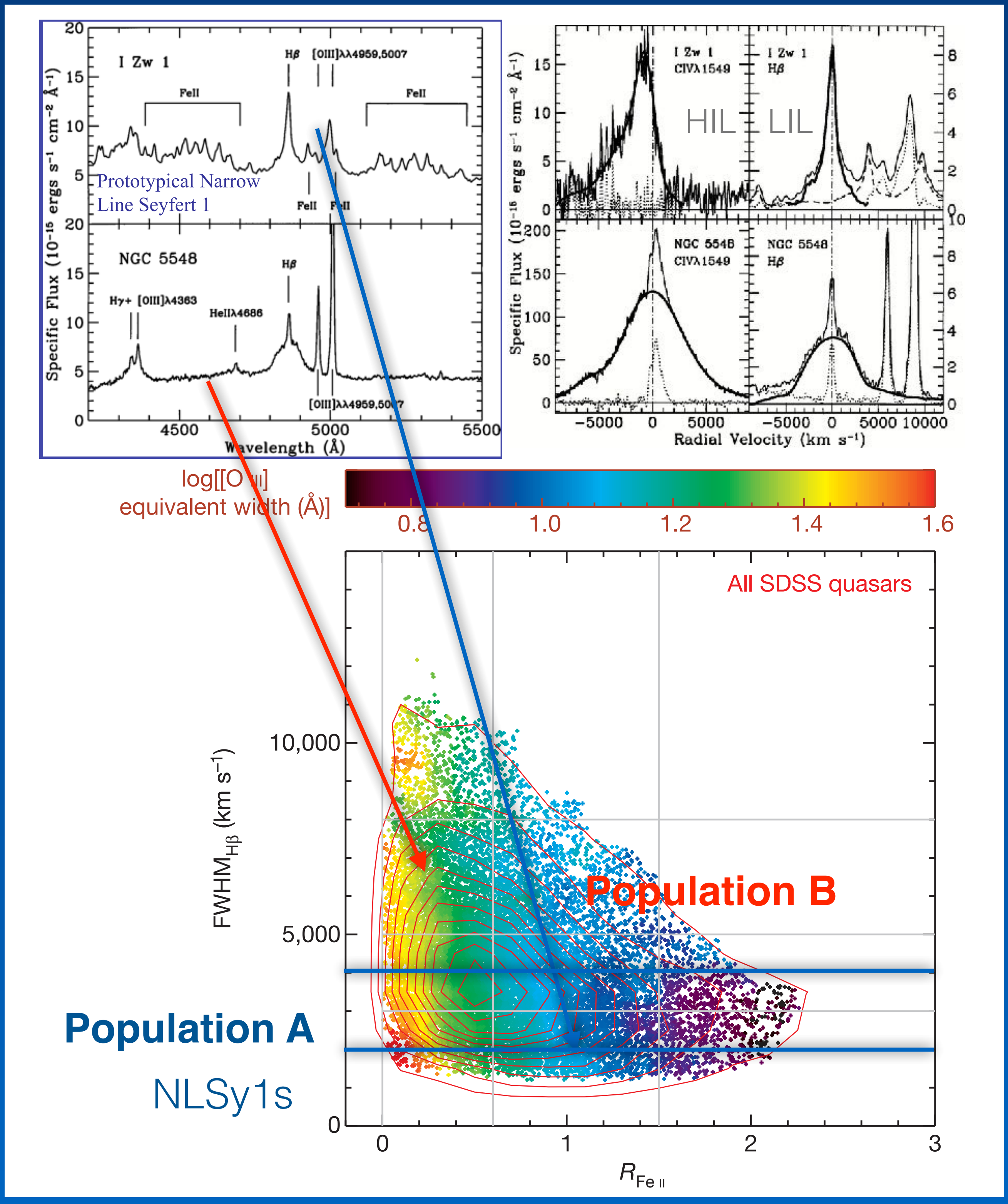

Multifrequency parameters related to the accretion process and the accompanying outflows show trends along the MS

Sulentic et al. 2000, 2011; Shen & Ho 2014; c.f. Du et al. 2016; Sniegowska et al 2020

Parameter	Population A	Population B	References
FWHM(Hβ_{BC})	800–4000 km s^{-1}	4,000–10,000 km s^{-1}	1, 2, 3, 4
R_{Fe}	0.7	0.3	1, 2
c($\frac{1}{2}$) CIVλ1549$_{BC}$	−800 km s^{-1}	−250/+70 (RQ/RL)	5, 6, 7, 8
Γ_S	Often large (> 2)	Rarely large (≈ 2)	2, 9, 4, 10
W(Hβ_{BC})	∼ 80 Å	∼ 100 Å	2
Hβ_{BC} profile shape	Lorentzian	Double Gaussian	11, 12, 13
c($\frac{1}{2}$) Hβ_{BC}	∼ zero	+500 km s^{-1}	13
SiIII]/CIII]	0.4	0.2	14, 15, 16
FWHM CIVλ1549$_{BC}$	(2–6) $\cdot 10^3$ km s^{-1}	(2–10) $\cdot 10^3$ km s^{-1}	5, 17
W(CIVλ1549$_{BC}$)	Few Å – ≈ 60 Å	∼ 100 Å	4, 6, 7
AI(CIVλ1549$_{BC}$)	−0.1	0.05	5
W([OIII]λ5007)	1–20	20–80	1, 18, 19
v_r([OIII]λ5007)	Negative / 0	∼ 0 km s^{-1}	4, 18, 19, 20
FIR color α(60, 25)	0–−1	−1–−2	21
X-ray variability	Extreme/rapid common	Less common	22, 23
Optical variability	Possible	More frequent/higher amplitude	24
Probability radio loud	≈ 3–4%	25%	4, 25
[illegible]	Extreme BALs	Less extreme BALs	26, 27
log density[1]	≳ 11	≳ 9.5	14, 28
log U[1]	−2.0/−1.5	−1.0/−0.5	14, 28
log M_{BH} [$M_\odot$]	6.5–8.5	8.0–9.5	7, 8, 29
L/L_{Edd}	≈ 0.2–1.0	∼ 0.01 – ≈ 0.2	1, 4, 7, 29, 30, 31

1: Boroson and Green (1992); 2: Sulentic et al. (2000a); 3: Collin et al. (2006); 4: Shen and Ho (2014), 5. Sulentic et al. (2007), 6: Baskin and Laor (2005); 7: Richards et al. (2011); 8: Sulentic et al. (2016); 9: Wang et al (1996); 10: Bensch et al. (2015); 11: Véron-Cetty et al. (2001); 12: Sulentic et al. (2002); 13: Marziani et al. (2003b); 14: Marziani et al. (2001); 15: Wills et al. (1999); 16: Bachev et al. (2004), 17: Coatman et al. (2016); 18: Zhang et al. (2011); 19: Marziani et al. (2016a); 20: Zamanov et al. (2002); 21: Wang et al. (2006); 22: Turner et al. (1999); 23: Grupe et al. (2001); 24: Giveon et al. (1999); 25: Zamfir et al. (2008); 26: Reichard et al. (2003); 27: Sulentic et al. (2006); 28: Negrete et al. (2012); 29: Boroson (2002); 30: Peterson et al. (2004); 31: Kuraszkiewicz et al. (2000).

Fraix-Burnet et al. 2017

Extreme Population B

very broad Balmer profiles, low R_{FeII}, low accretion rate

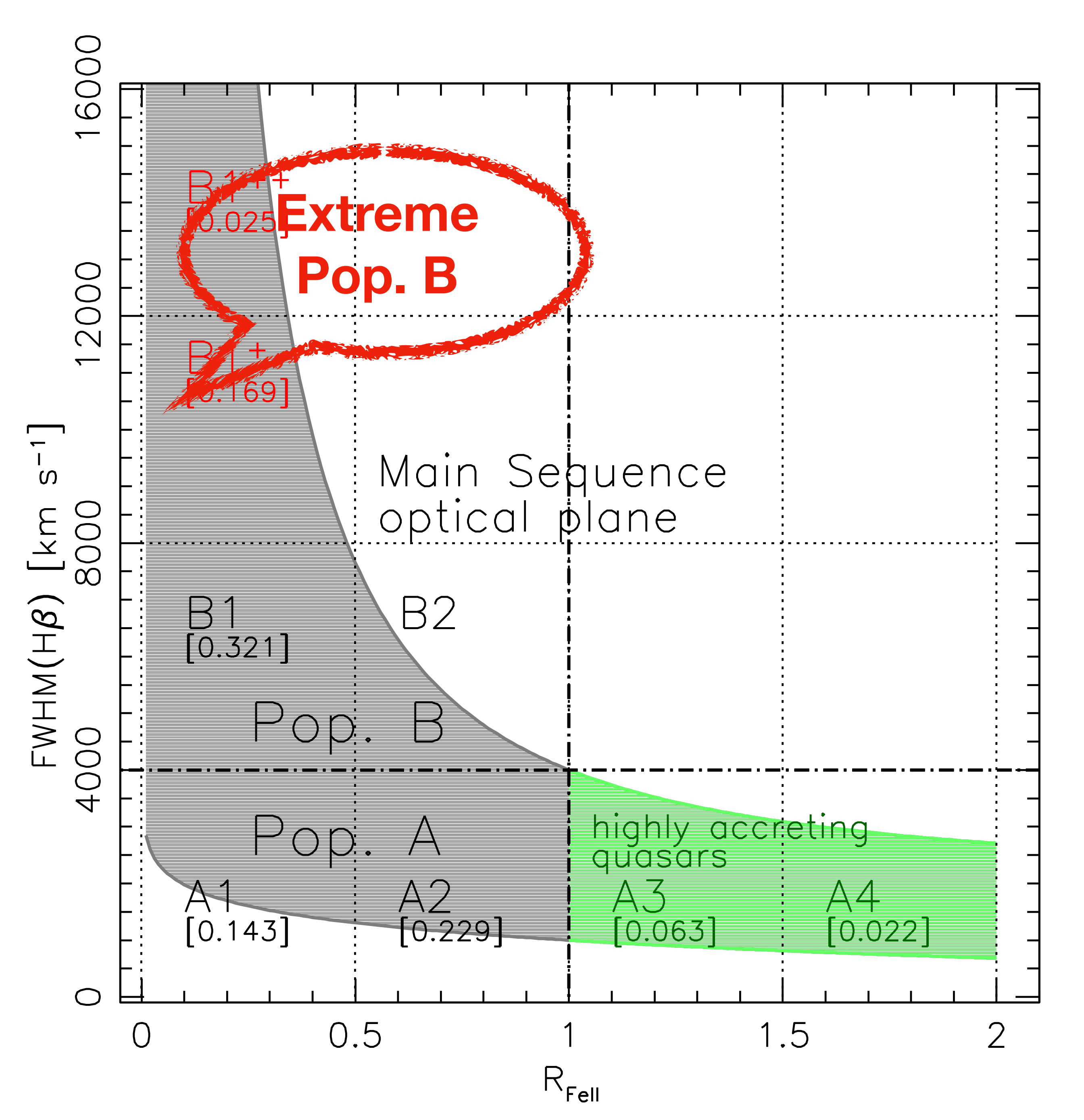

MS correlates: extreme Population B

Extreme Population B: few (<10% in SDSS), very broad Balmer profiles suggest accretion disk or binary BLR; frequently "changing look" low Eddington ratio ≪ 0.1

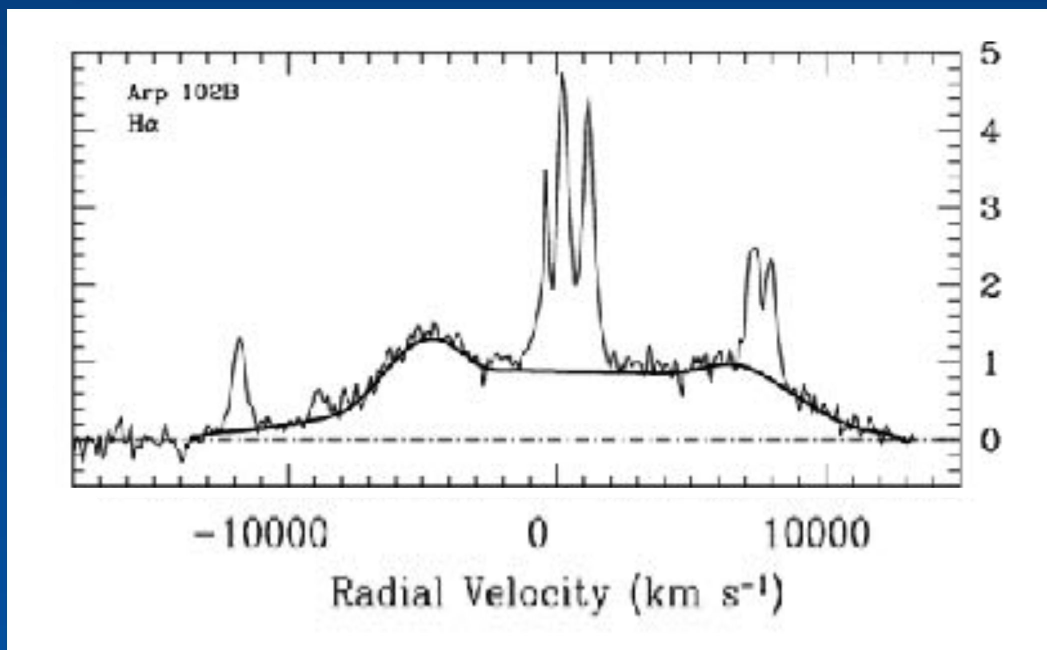

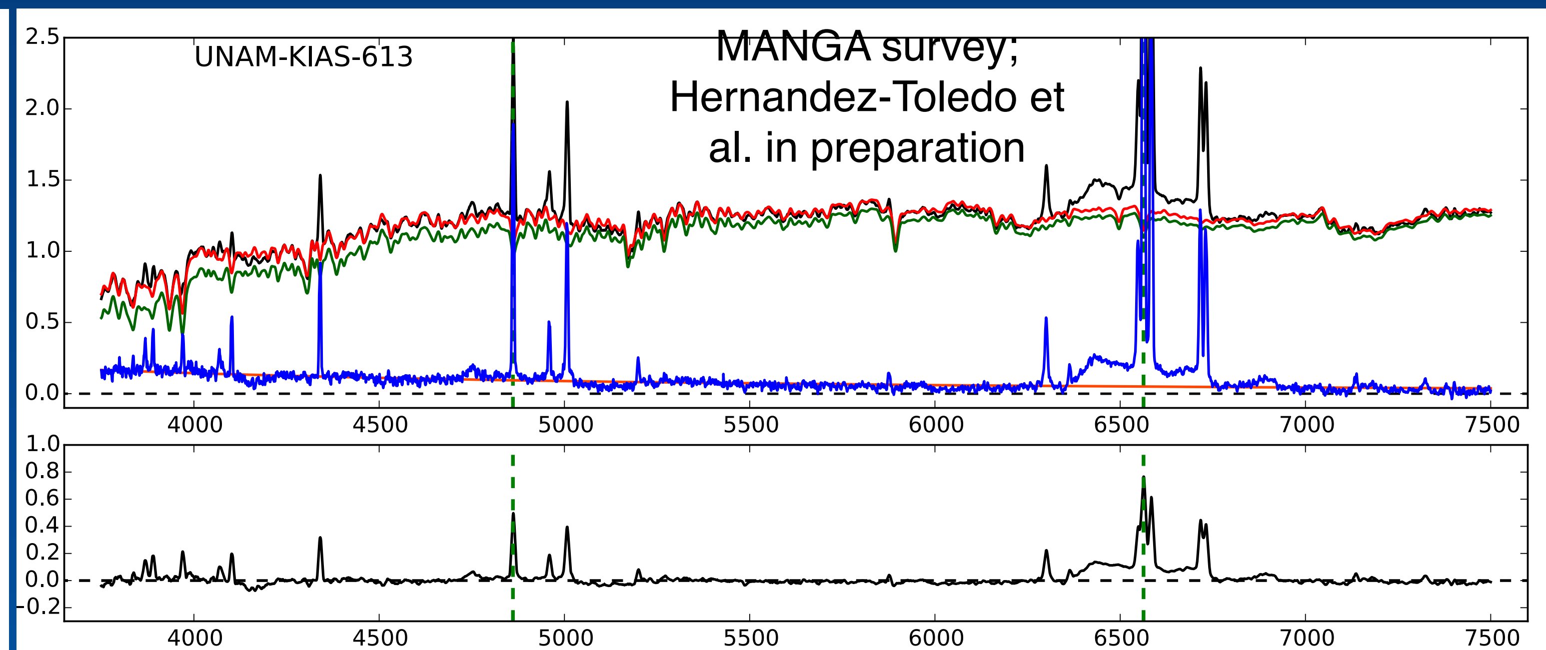

$M_R \sim -25.7$ $R_{FeII} \lesssim 0.1$ $L/L_{Edd}<0.1$

$M_z > -21.9$ $R_{FeII} \lesssim 0.1$ $L/L_{Edd} \ll 0.1$

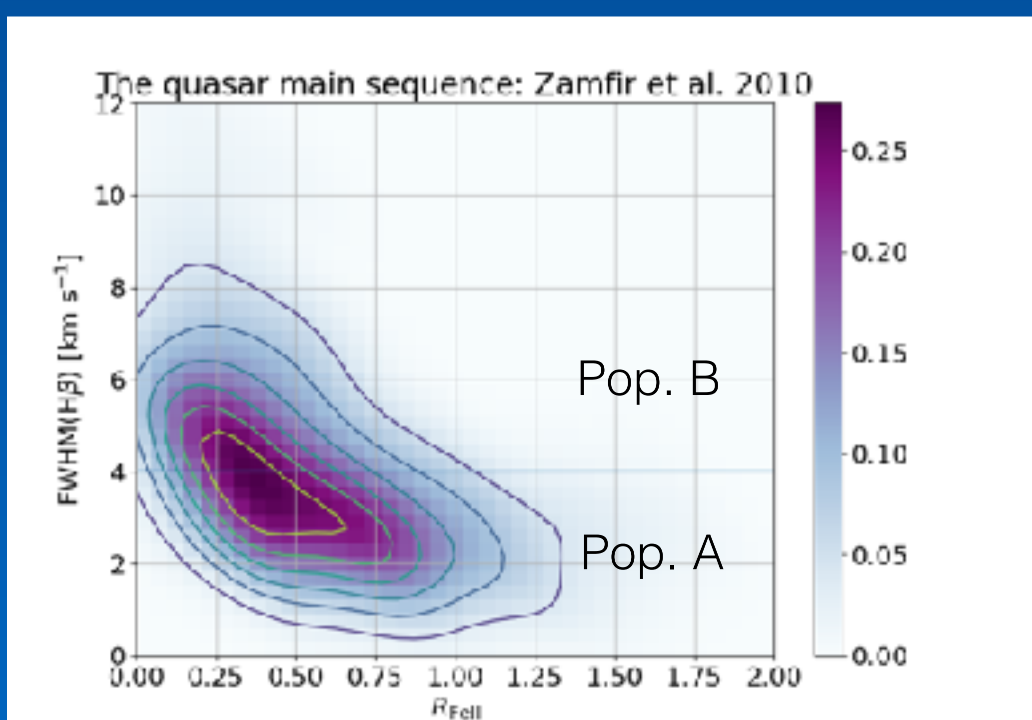

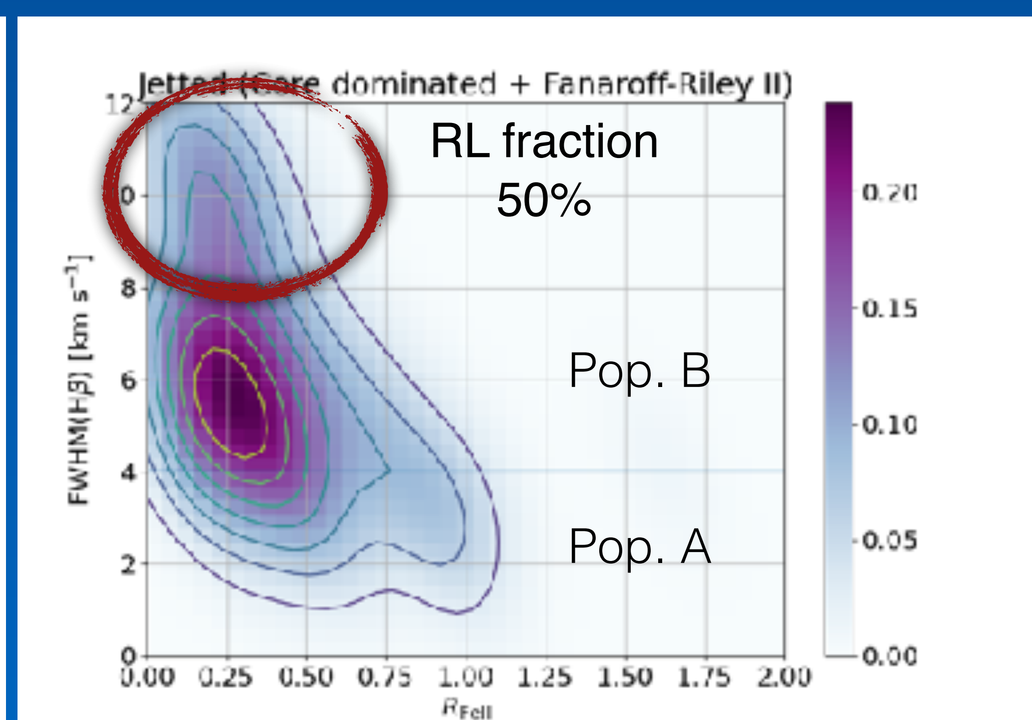

Jetted sources predominantly confined to Pop. B; high RL fraction for FWHM Hβ > 8000 km/s

Sulentic et al. 2000; Strateva et al. 2003, 2007; Ganci et al. 2019, Marziani et al. 2021

MS correlates — The HIL CIλ1549 profile

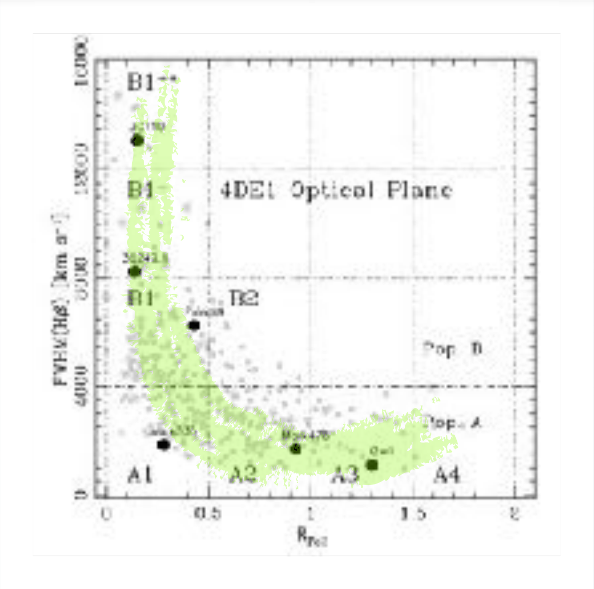

The CIVλ1549 line profile:
scaled symmetric Hβ from + excess blueshifted emission
"virialized" BLR + outflow/wind component

e.g., Leighly 2000, Bachev et al. 2004, Marziani et al. 2010; Denney et al. 2012; low-z FOS/HST data

Virialized: profile symmetric and unshifted with respect to rest frame

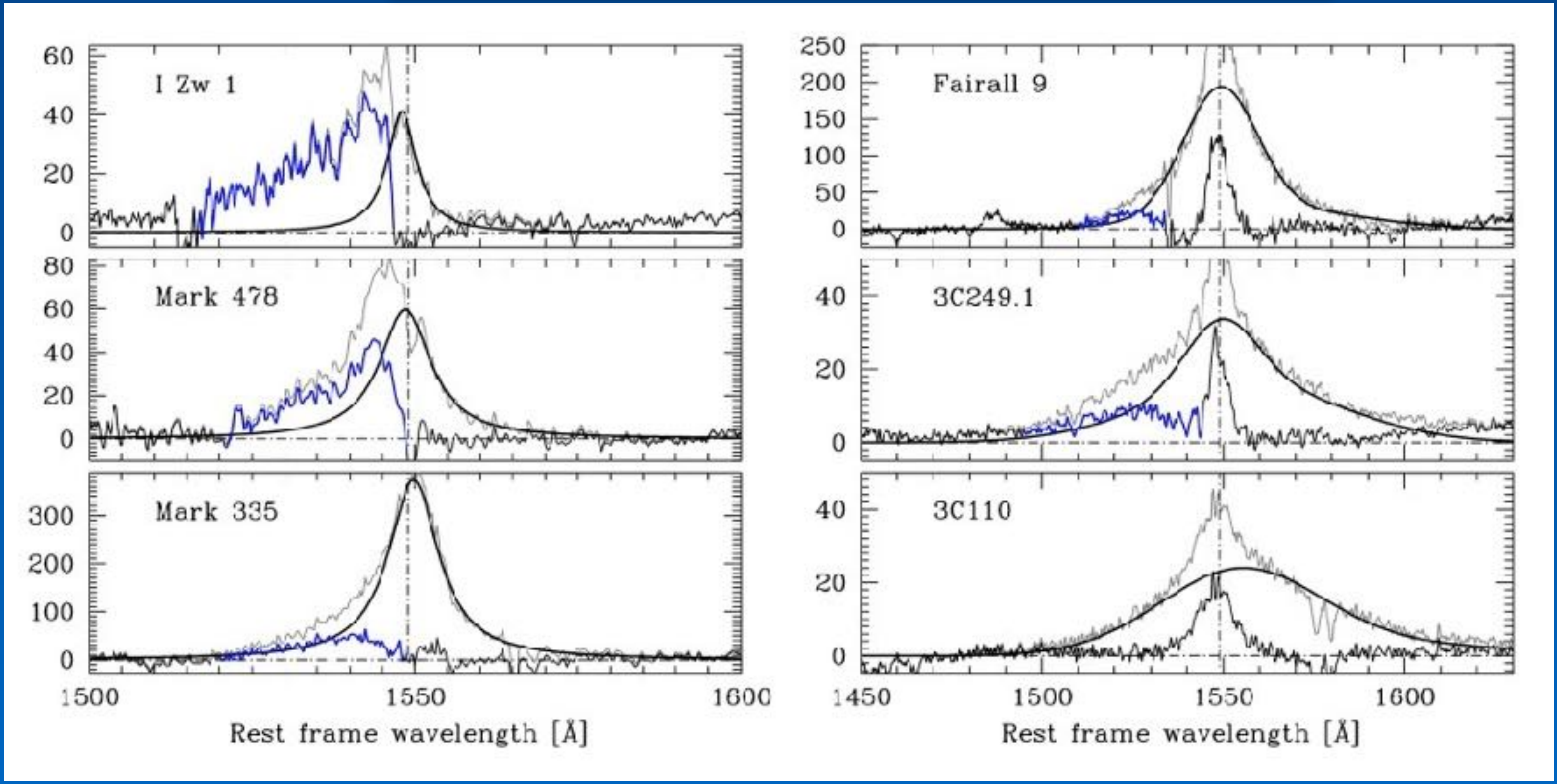

MS correlates — CIV shifts in the optical plane of E1

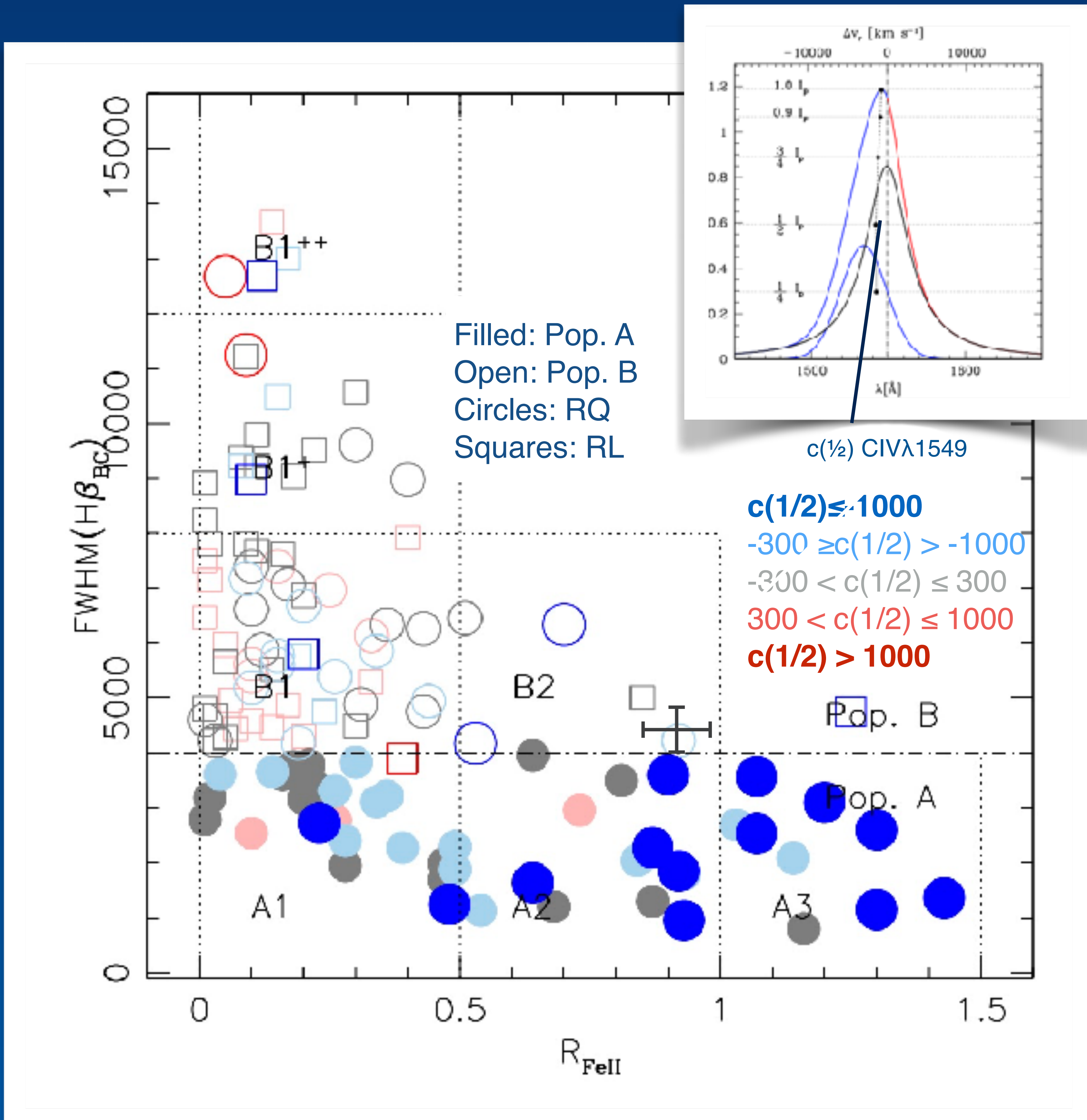

Large shift of CIVλ1549 centroid at ½ along the MS are found for FWHM(Hβ)< 4000 km s^{-1}

“discontinuity” at FWHM(Hβ) ≈ 4000 km s^{-1} suggested by the Hβ profile shape change

Marziani & Sulentic 2012; Sulentic et al. 2007; low *z* sample UV FOS data

MS correlates — CIV shifts in the optical plane of E1

Outflowing gas coexists with a virialized system emitting mainly LILs, even at the highest luminosity

Virialized: profile symmetric and unshifted with respect to rest frame

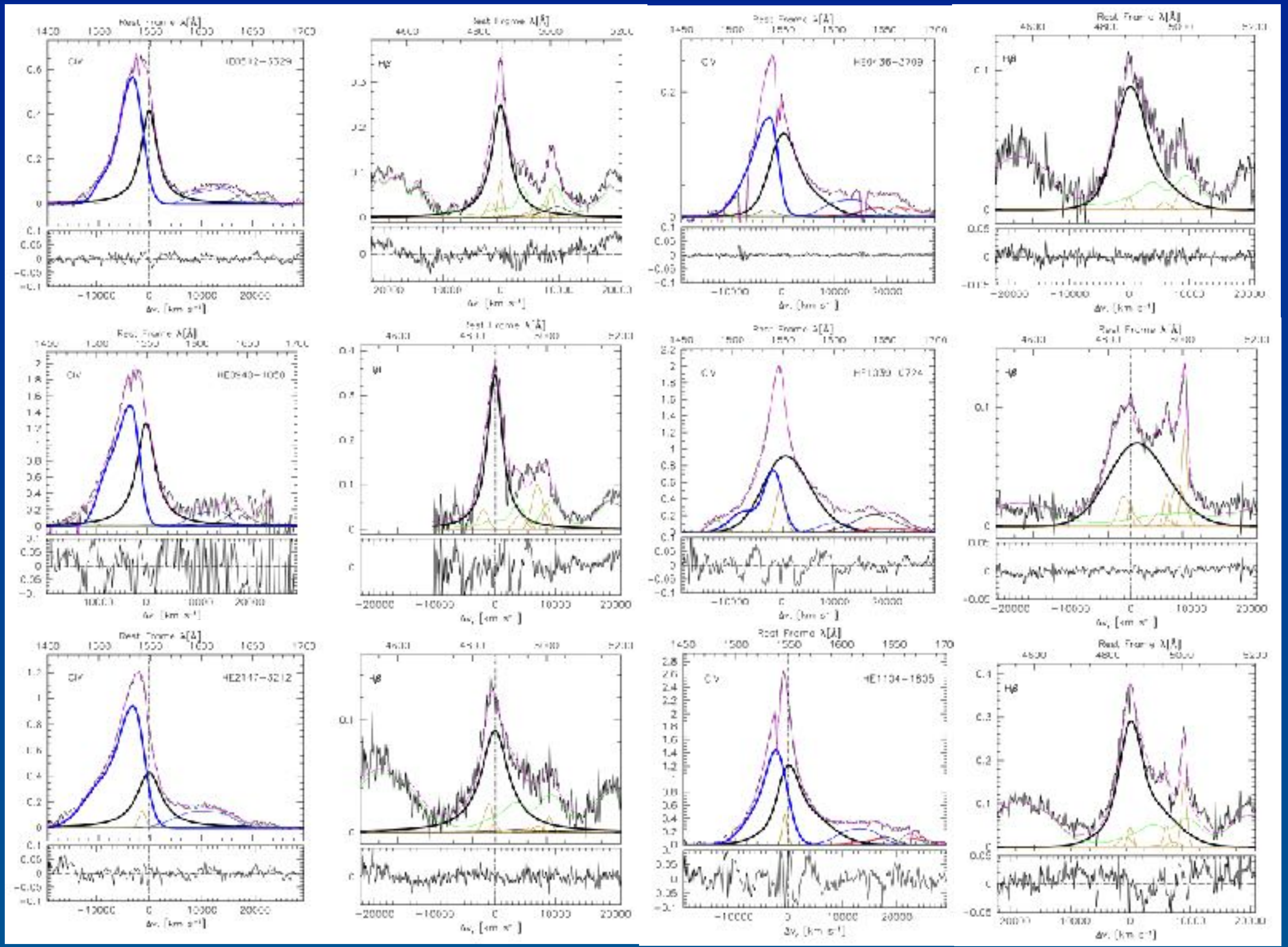

Hamburg-ESO luminous quasars
$L>10^{47}$ erg s^{-1} at $z\sim1.5$, e.g., Sulentic et al. 2017; see also Bischetti et al. 2017; Vietri et al. 2018

MS correlates — CIV shifts in the optical plane of E1

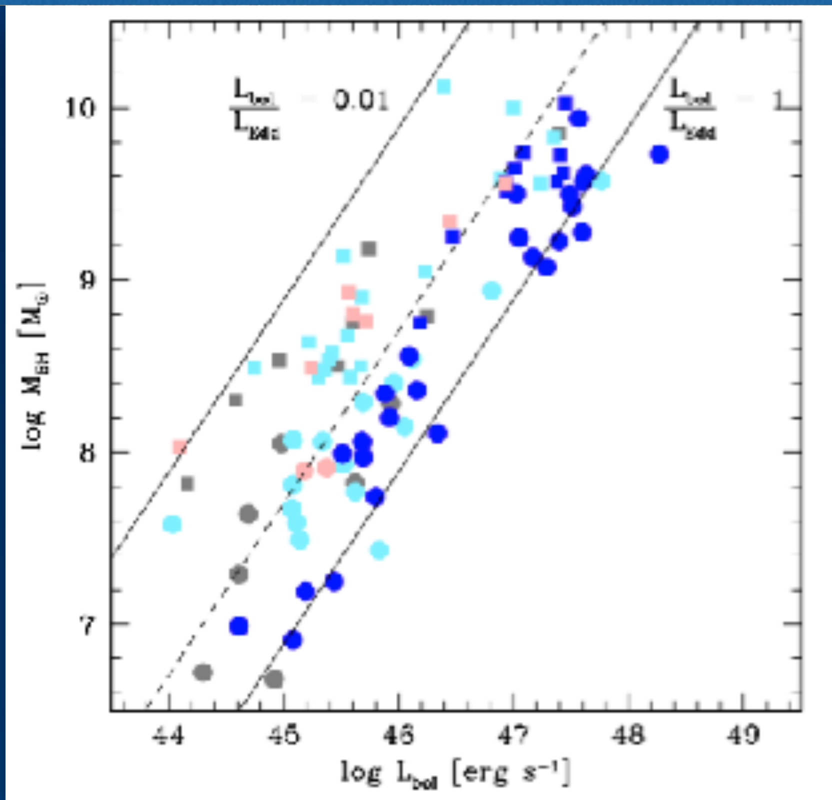

CIV blueshifts are a largely self-similar phenomenology over 3-4 orders of magnitude in quasar luminosity and black hole mass

Largest CIVλ1549 blueshifts are observed at high L/L_{Edd} but not necessarily at high M_{BH} or high L

FOS + high L HE sample (28 objects) Sulentic et al. 2017

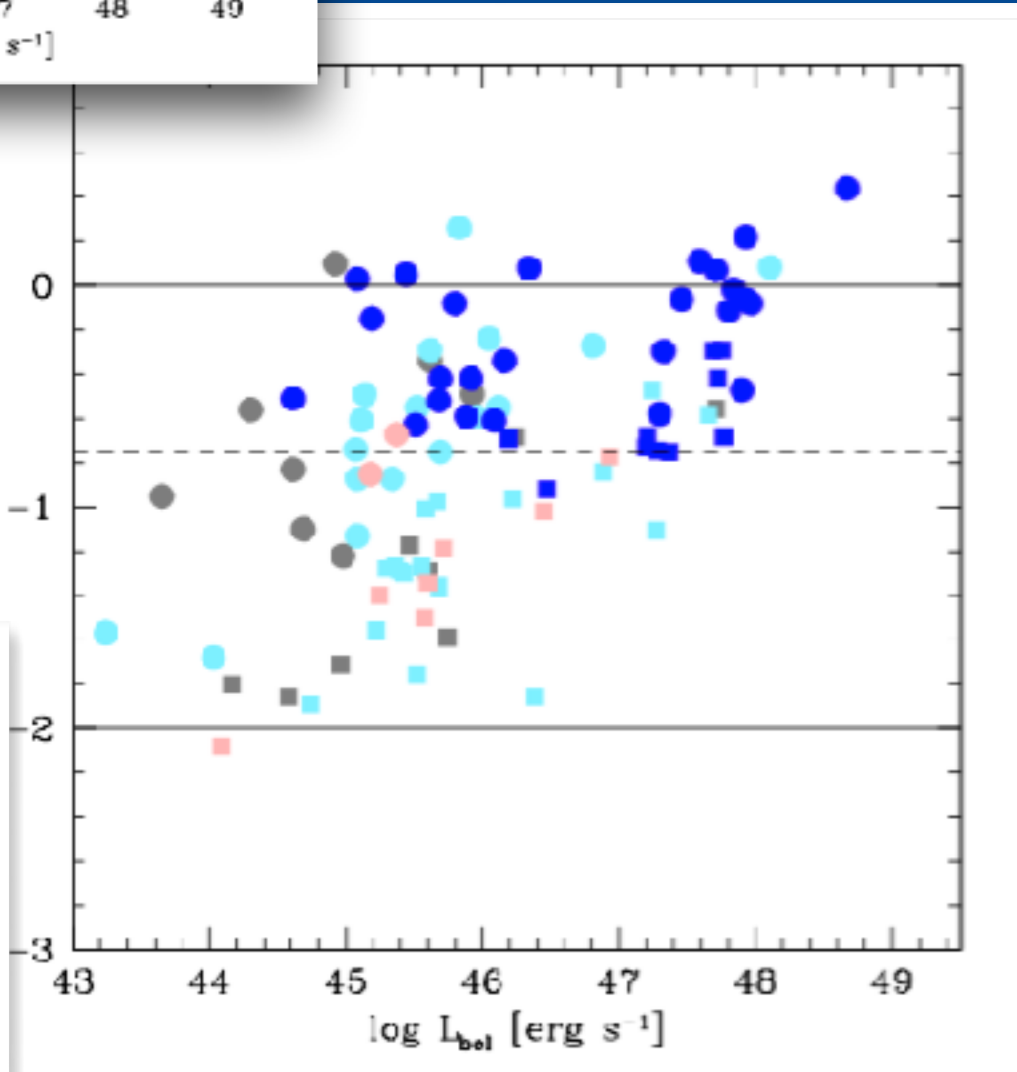

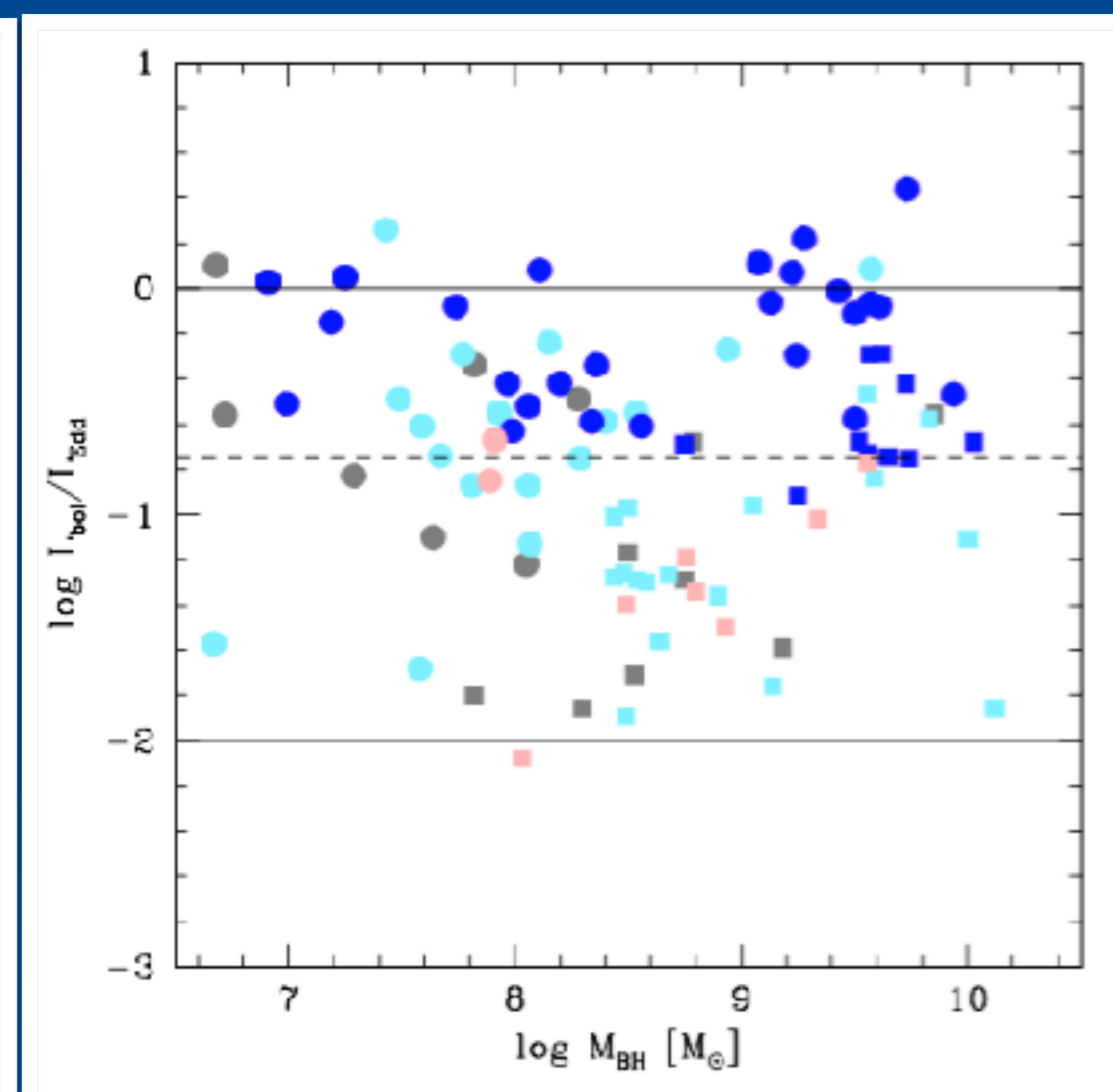

c(1/2)≤-1000
-300 ≥c(1/2) > -1000
-300 < c(1/2) ≤ 300
300 < c(1/2) ≤ 1000
c(1/2) > 1000
Circles: Pop. A
Squares: Pop. B

Balance between gravitation and radiation forces

Example: Compton thin slab absorbing all of the ionizing continuum

$$n_{\mathrm{H}} \propto r^{-s} \quad 1 \leqslant s \leqslant 5/2$$

$$N_{\mathrm{col}} \propto r^{-2s/3}$$

$$\text{Eddington ratio} = \frac{L_{\mathrm{bol}}}{L_{\mathrm{Edd}}} \propto \frac{L_{\mathrm{bol}}}{M_{\mathrm{BH}}}$$

$$\frac{a_{\mathrm{rad}}}{a_{\mathrm{grav}}} \approx 0.088 L_{44} M_{\mathrm{BH}}^{-1} N_{\mathrm{c},23}^{-1}$$

$$\frac{a_{\mathrm{rad}}}{a_{\mathrm{grav}}} \approx 7.2 \frac{L_{\mathrm{bol}}}{L_{\mathrm{Edd}}} N_{\mathrm{c},23}^{-1}$$

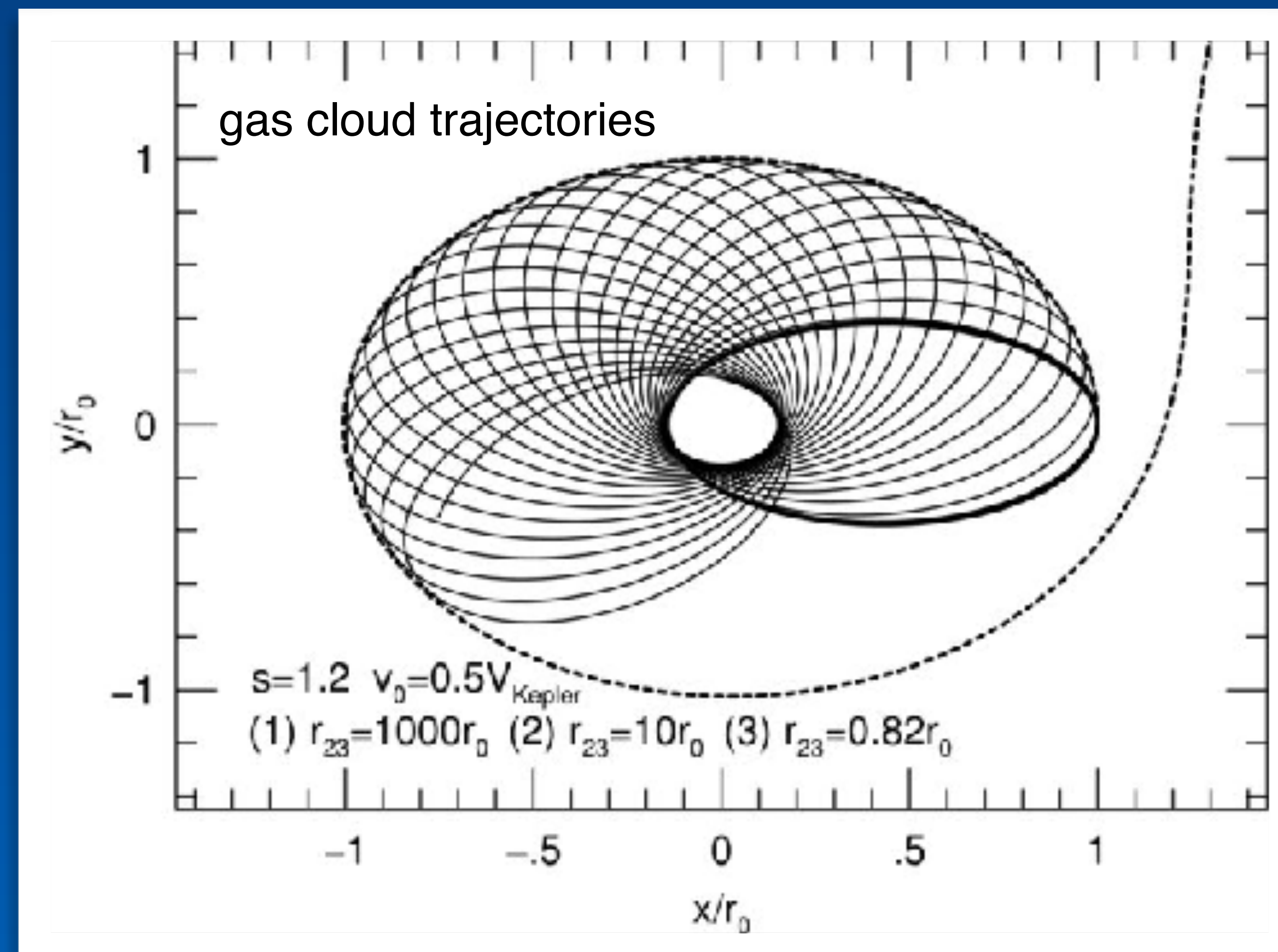

Ferland et al. 2009; Marziani et al. 2010; Netzer & Marziani 2010

Blueshifted component: low N_c gas may become unbound
Broad Component stable (virial)

MS — L/L_{EDD} as the MS driver

Interpretation of the optical MS plane at low-z in terms Eddington ratio and orientation

Population A: $L/L_{Edd} \gtrsim 0.1$-0.2
includes rare ($P(\theta) \propto \sin\theta$) low L/L_{Edd} sources observed almost face-on;
NLSy1s preferentially sample face-on sources along the MS

Virial velocity field in a flattened geometry

$M_{BH} = f(\theta) r_{BLR}\, FWHM^2/G$
$f(\theta) = 1/[4(\kappa^2+\sin^2\theta)]$

$\delta v_K^2 = f(\theta) FWHM^2$
$\kappa = \delta v_{iso}/\delta v_K$

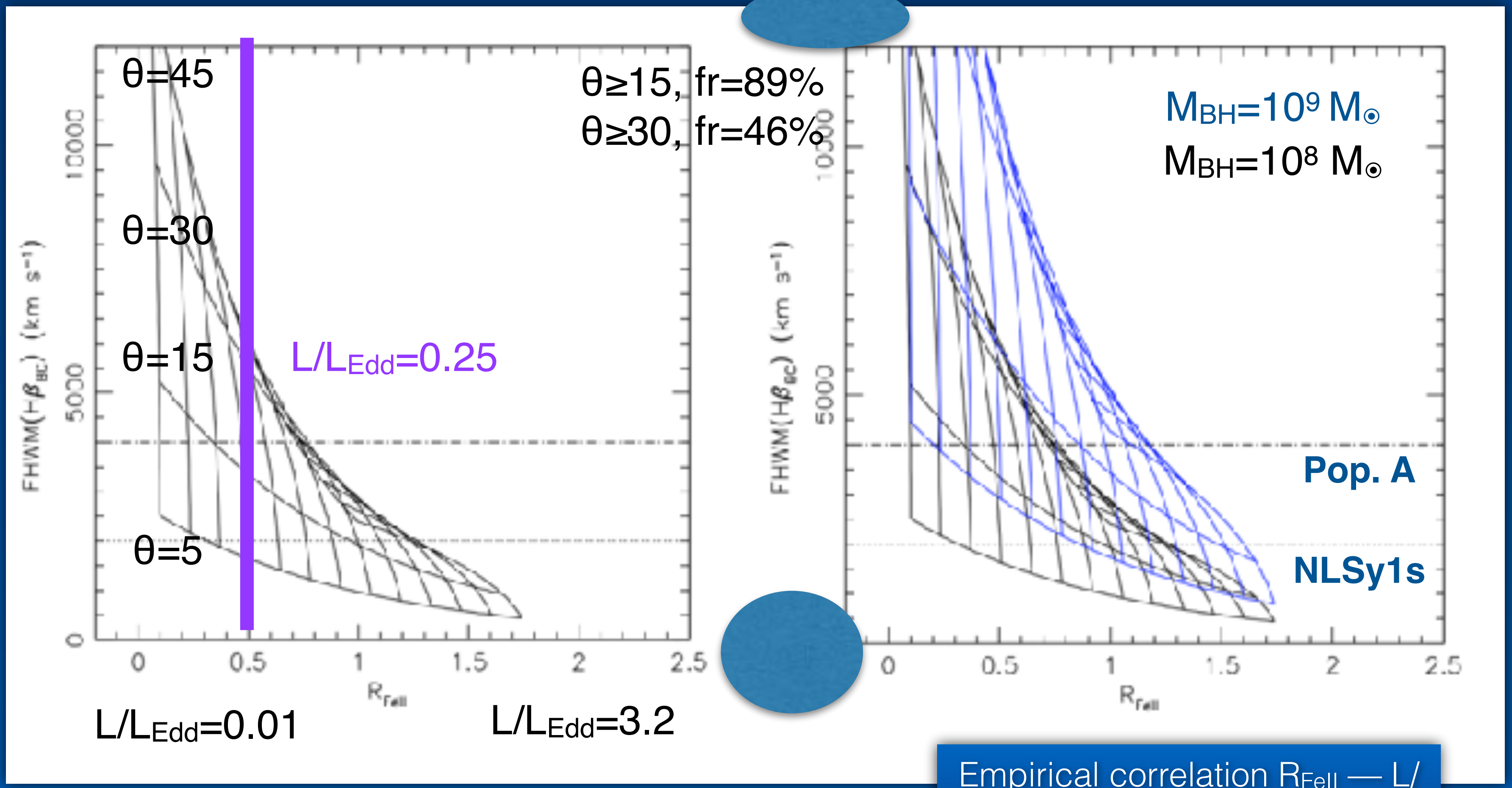

Empirical correlation R_{FeII} — L/L_{Edd} of Du et al. (2016)

Key assumptions: $R_{FeII} \propto L/L_{Edd}$

$FWHM \propto M_{BH}^{1/4} (L/L_{Edd})^{-1/4} f(\theta)^{-1/2}$ (virial);
$R_{FeII} \propto R_{FeII}(L/L_{Edd}) \cos\theta\, (1+ b \cos\theta)$

Marziani et al. 2001; Marziani et al. 2018

The relative occupation in the $R_{Fe\,II}$ sequence *is* explained as a sequence of increasing L/L_{Edd} and related observational trends i.e., cloud density n_H, chemical composition Z, and SED shape.

B and A1: relatively low density, low Z, and low L/L_{Edd}
A2: moderate density $n_H \sim 10^{11}$ cm^{-3}, intermediate L/L_{Edd}, $Z \sim 5Z_\odot$
$R_{FeII} > 1$: higher n_H, radiative output at the $L/L_{Edd} \sim 1$, and $Z \gtrsim 10Z_\odot$

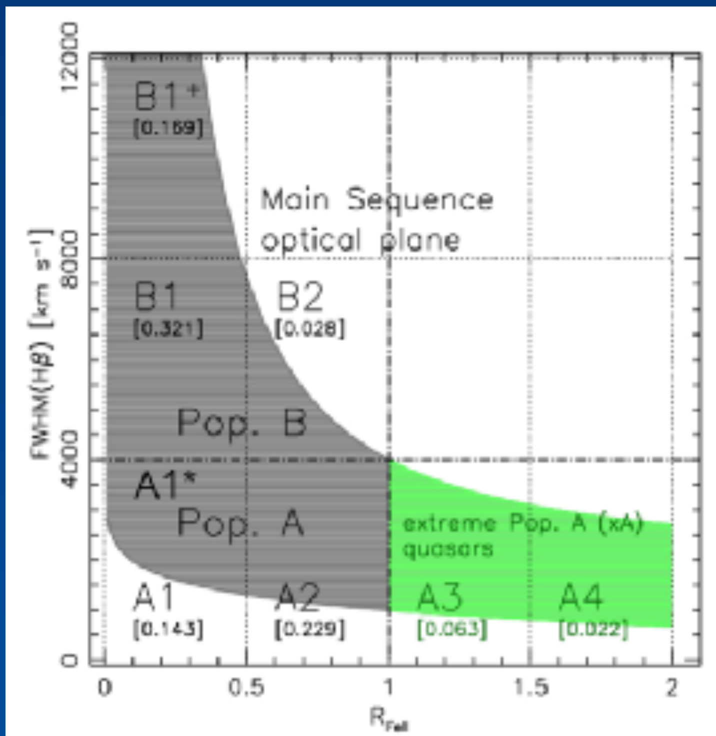

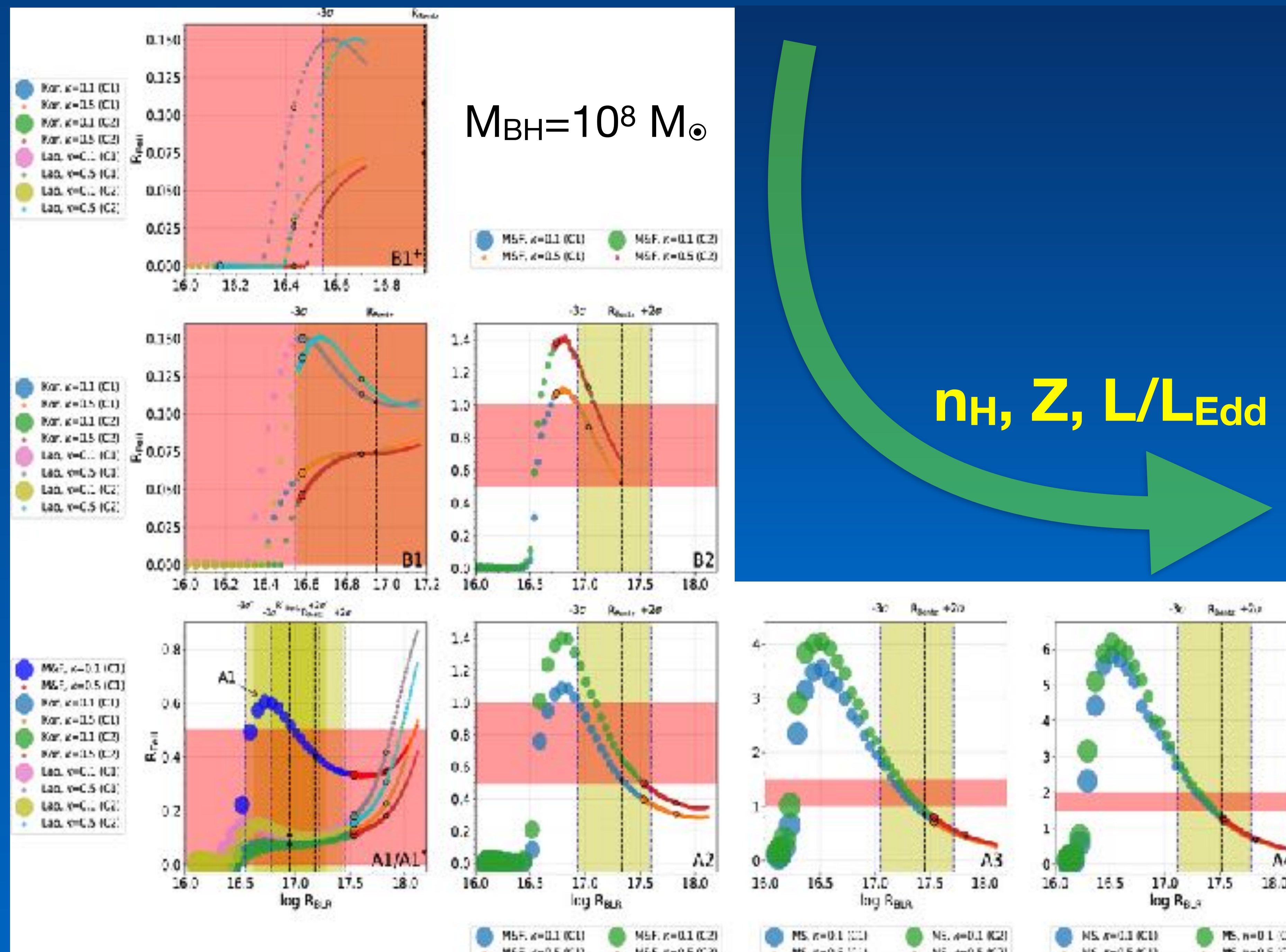

R_{FeII} predicted from Cloudy 17.02 models as a function of R_{BLR}

Panda et al. 2019

Population B, Population A, xA in different accretion modes
Pop B.: geometrically thin, optically thick disk
Pop. A: inner geometrically thick
xA: full

Interplay between the Broad Line Region and different accretion modes?

D'Onofrio et al. 2021; Giustini and Proga 2019

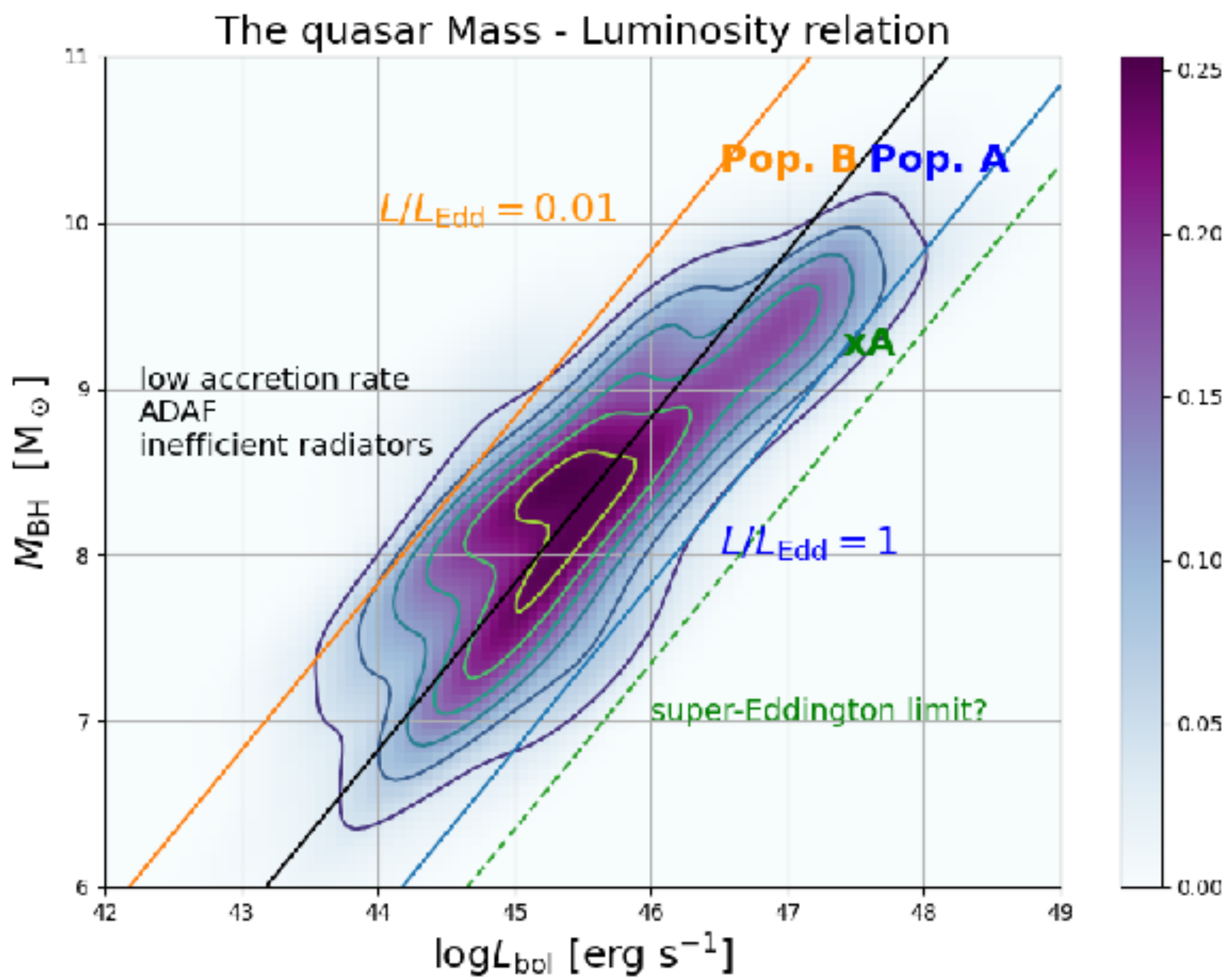

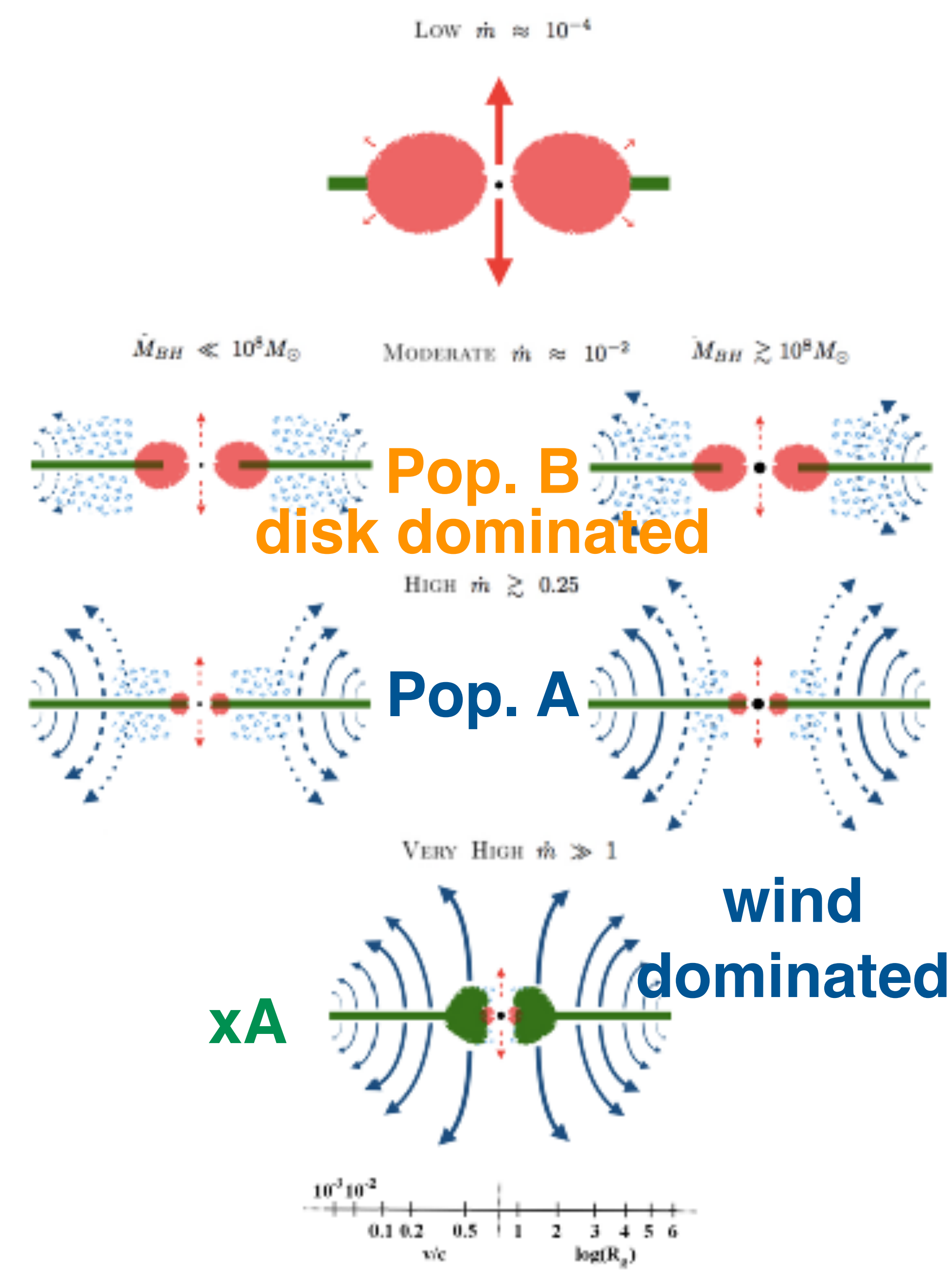

Extreme Population A

Highly accreting, possibly super-Eddington quasars

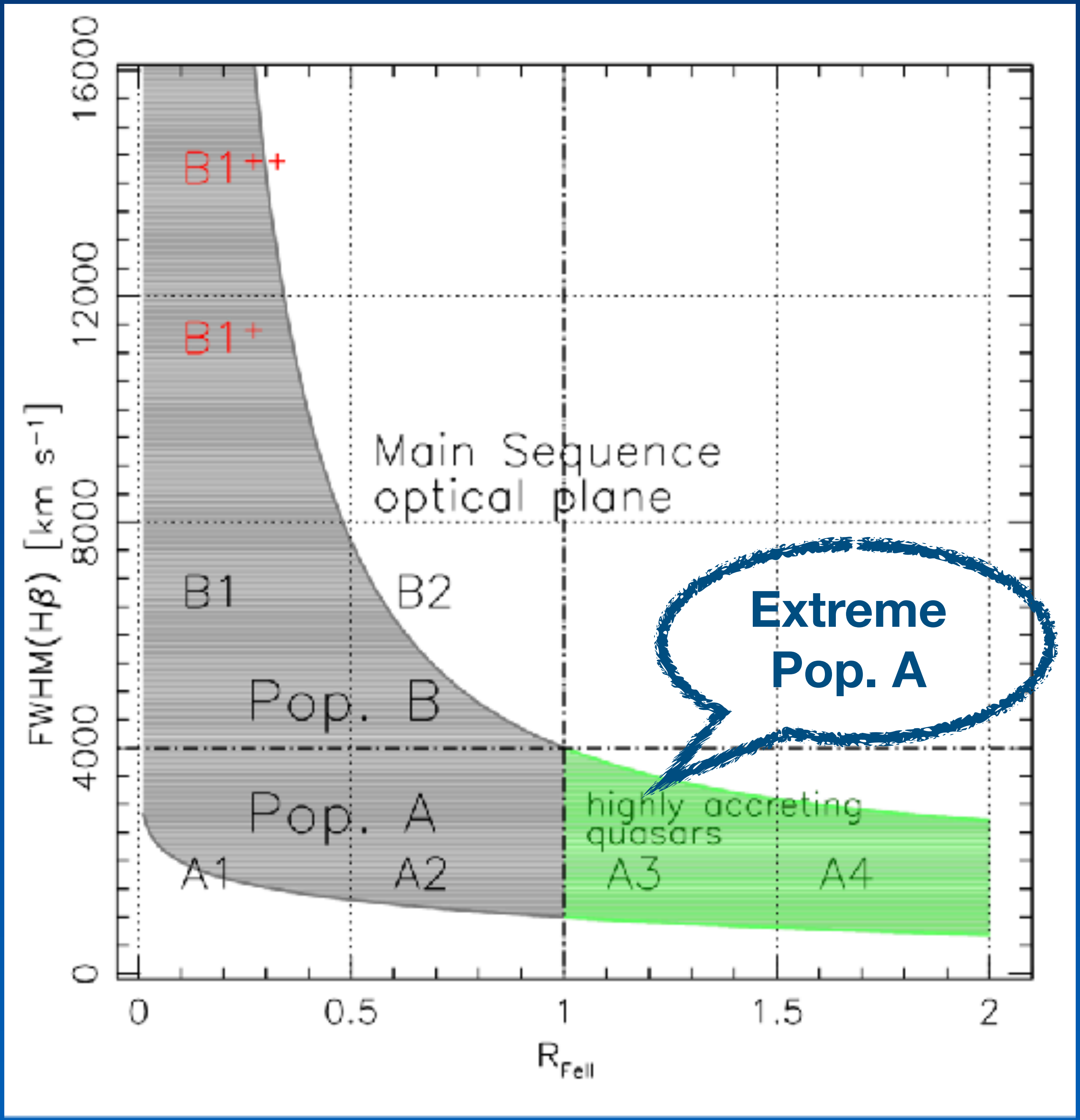

Extreme Population A — Selection and physical conditions

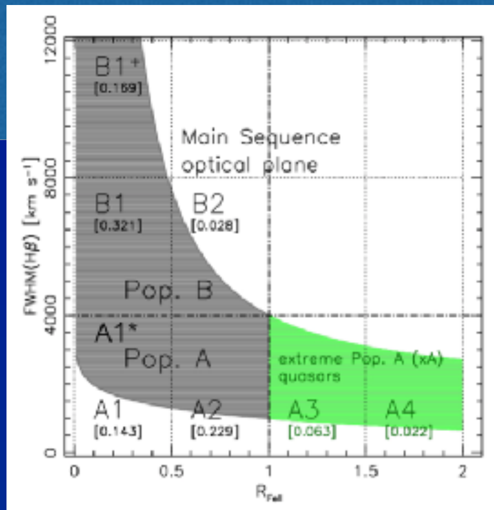

The UV spectrum of xA quasars

Martínez-Aldama et al. 2018

Symmetric low-ionization and blueshifed high-ionization lines even at the highest luminosity

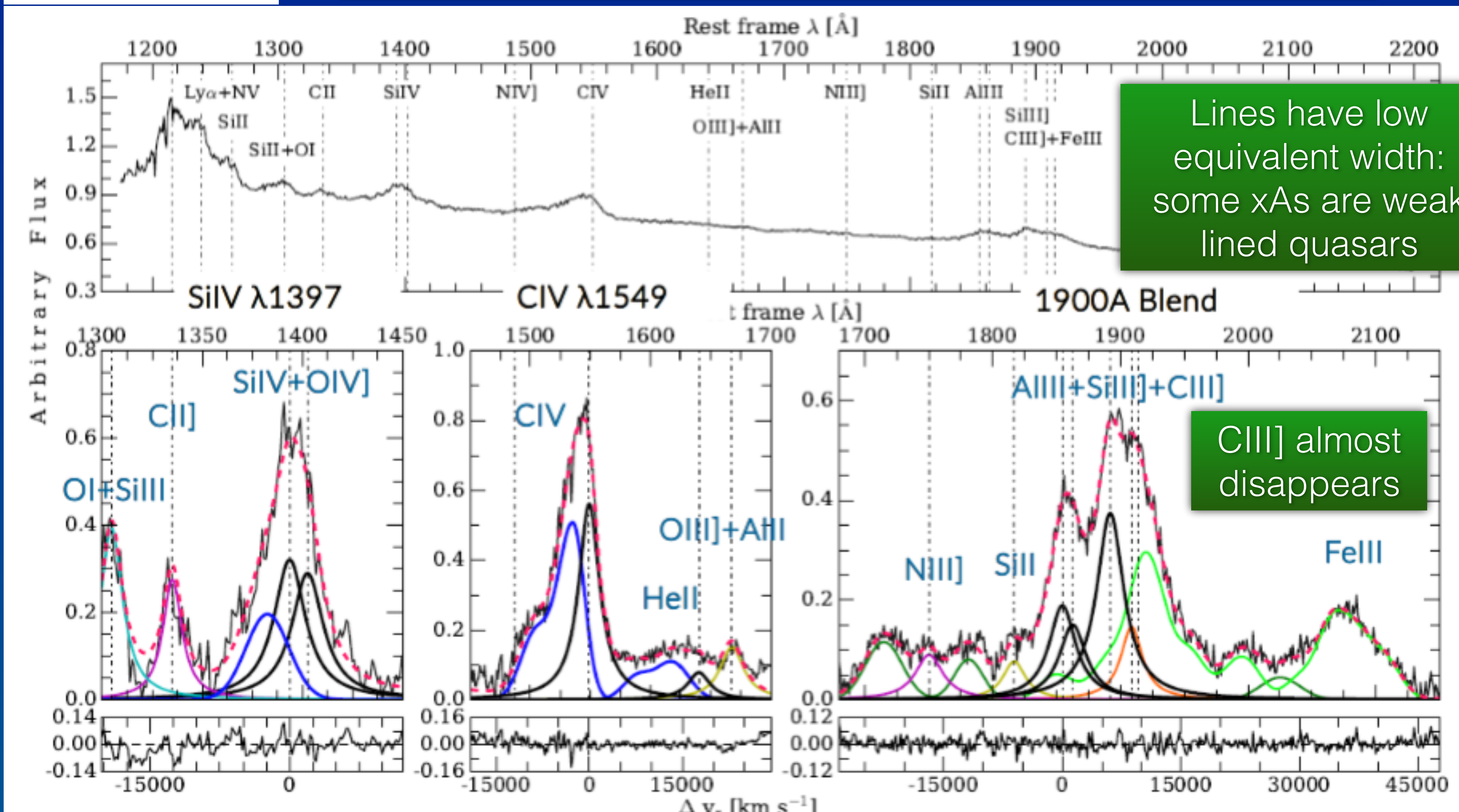

Lines have low equivalent width: some xAs are weak lined quasars

CIII] almost disappears

The diagnostics applied to xA spectra show a fairly monotonic trend with metallicity Z

Diagnostic line ratios
CIVλ1549/HeIIλ1640
AlIII λ1860/HeIIλ1640
(SiIV+OIV])λ1400/HeIIλ1640

HeIIλ1640 expedient because of of simple HeIIλ1640 radiation transfer

Arrays of CLOUDY 17.02 simulations covering the U, n_H parameter plane with a step of 0.25 dex, for -2 1$Z_\odot$ ≲ Z ≲ 1000 $Z_\odot$

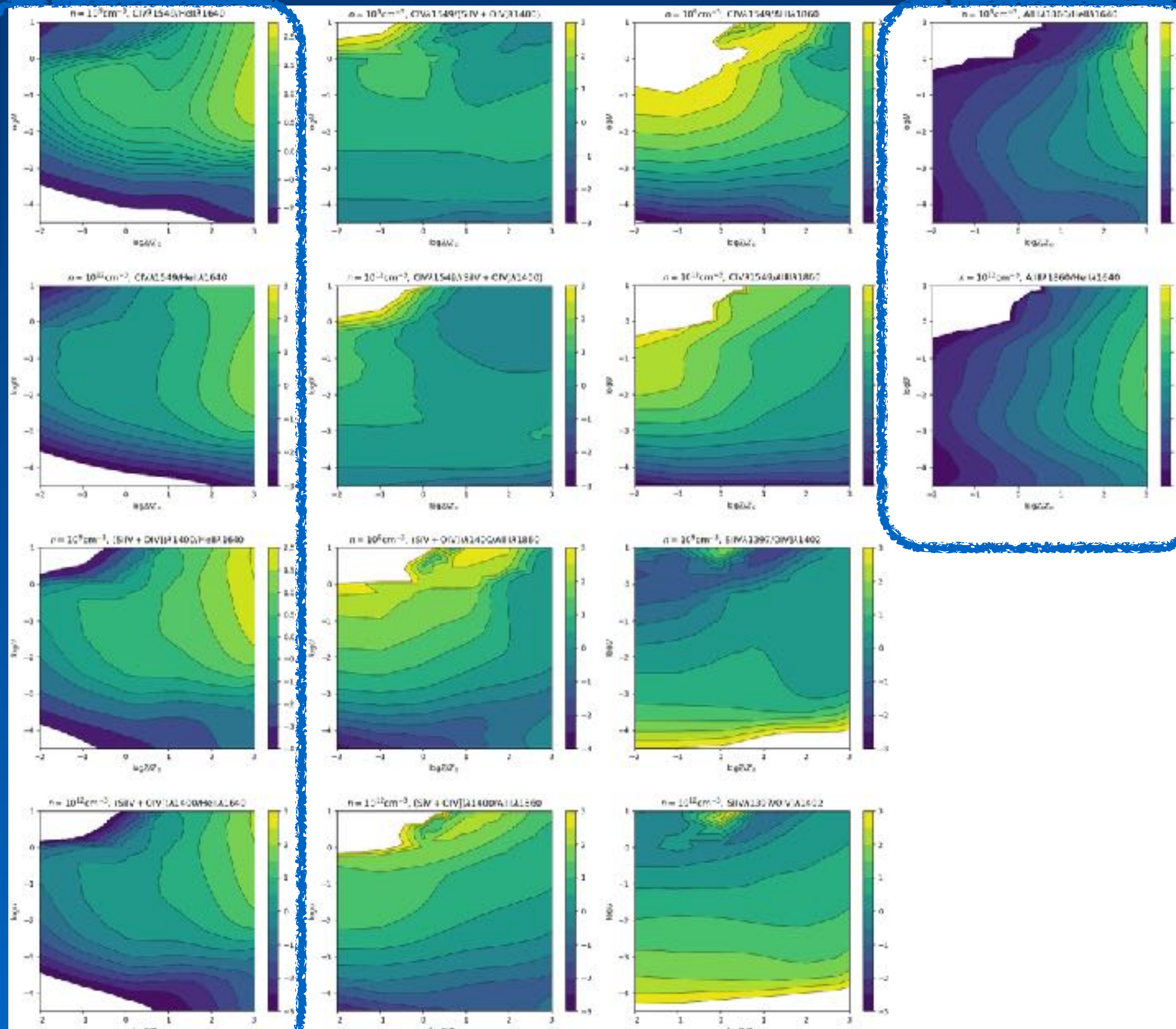

Sniegowska et al. 2021

Extreme Population A — Selection and physical conditions

Extreme values of metallicity (Z>20 Z⊙) with small dispersion

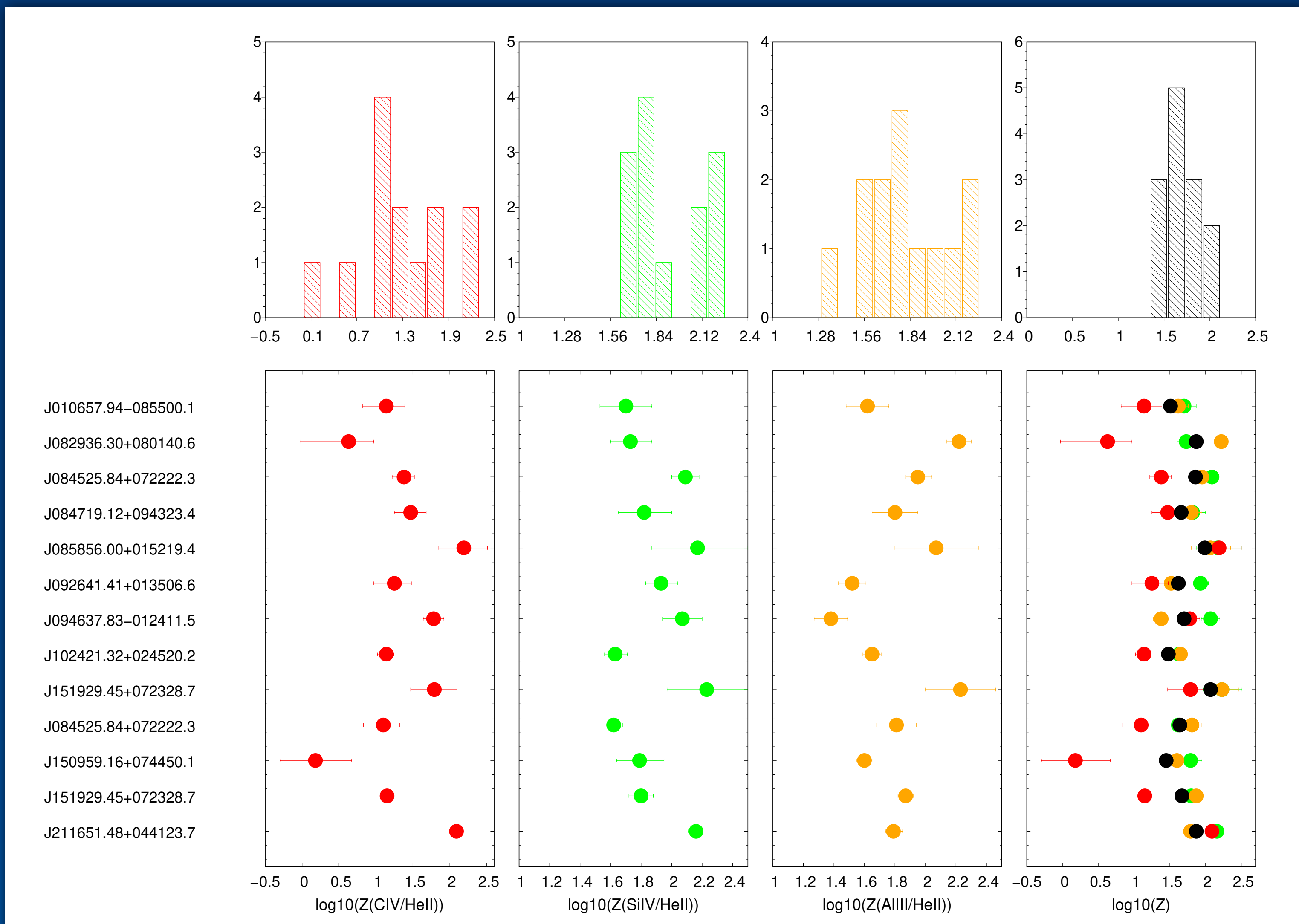

(Negrete et al. 2012; Martínez-Aldama et al. 2018; Sniegowska et al. 2021)

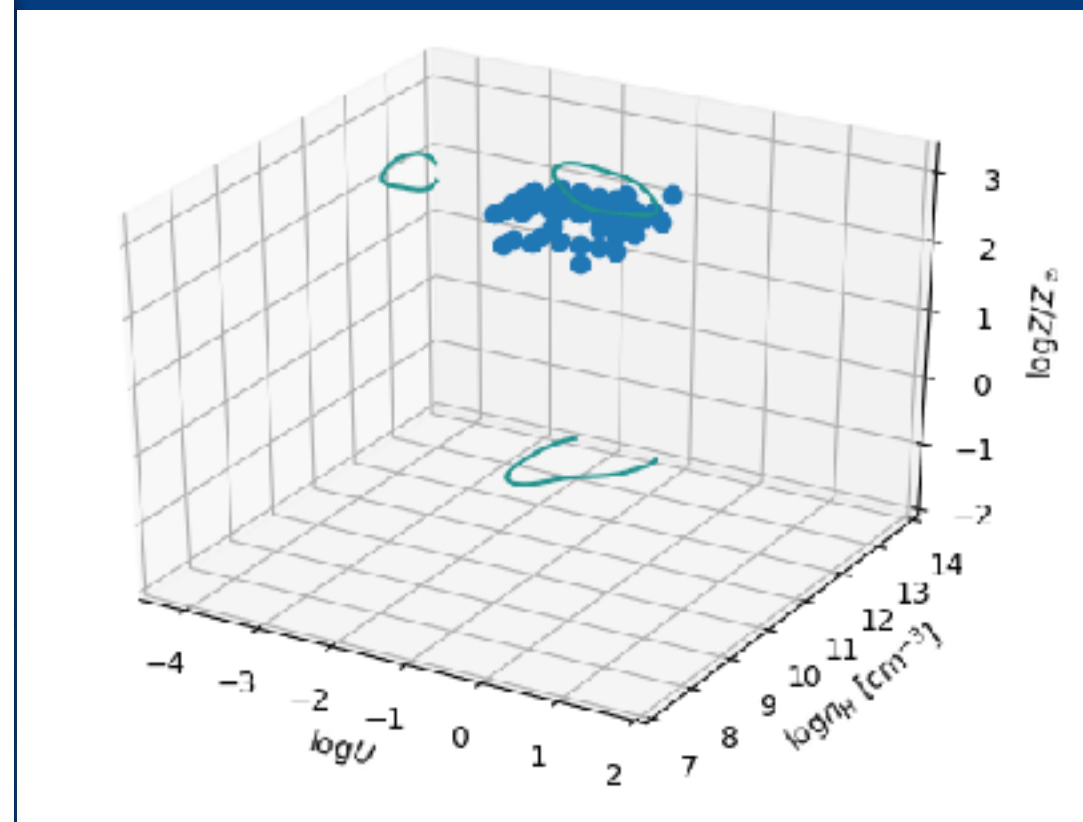

For the low-ionizaton BLR, ionization parameter, density, and Z are constrained

Important caveat: relative elemental abundances scaling as solar

The xA can reach very high radio power $P_\nu \sim 10^{25}$ W Hz^{-1}

xA follows the correlation SFR from FIR - SFR from radio observed for radio-quiet quasars: radio power from supernova remnants

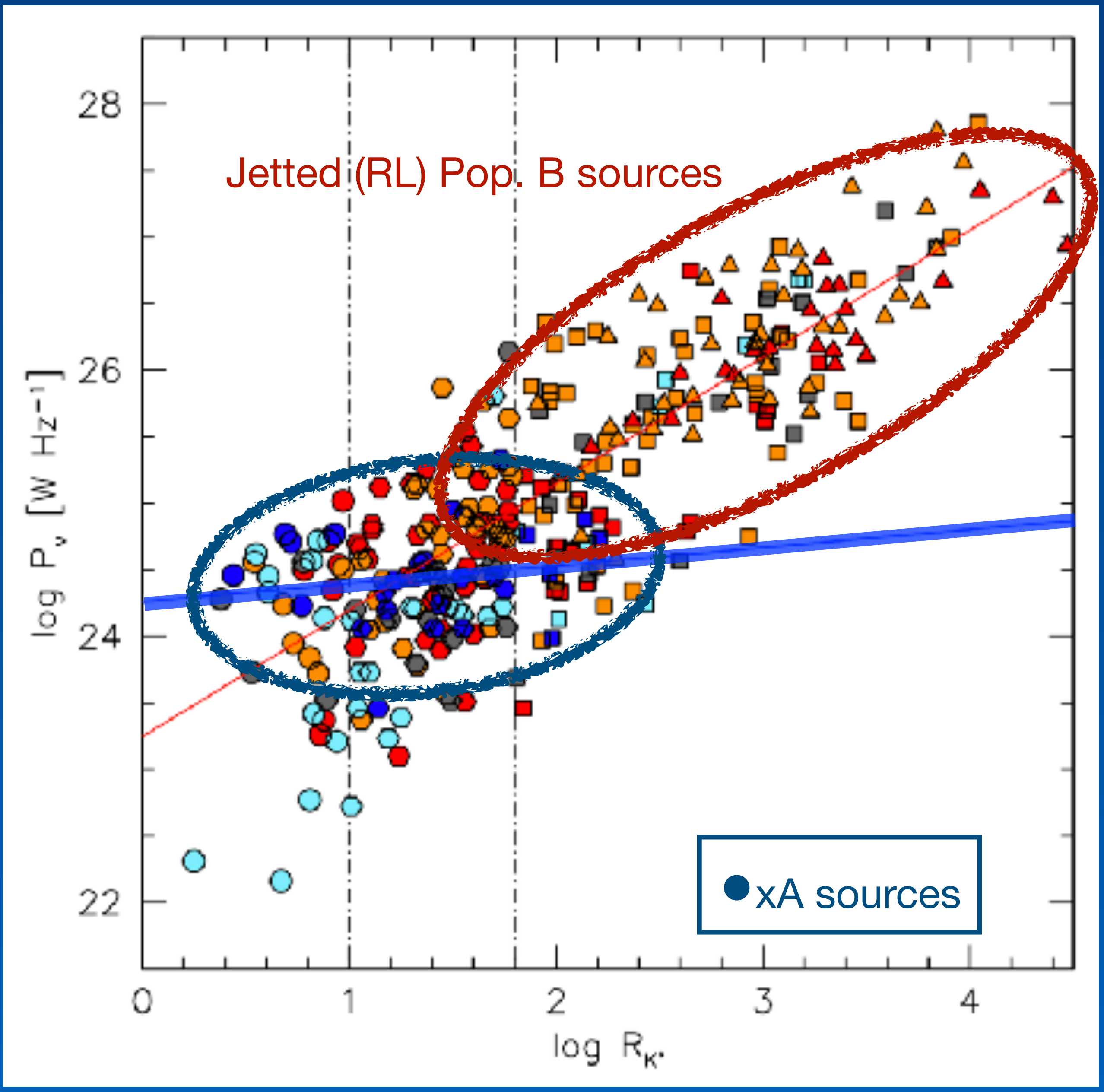

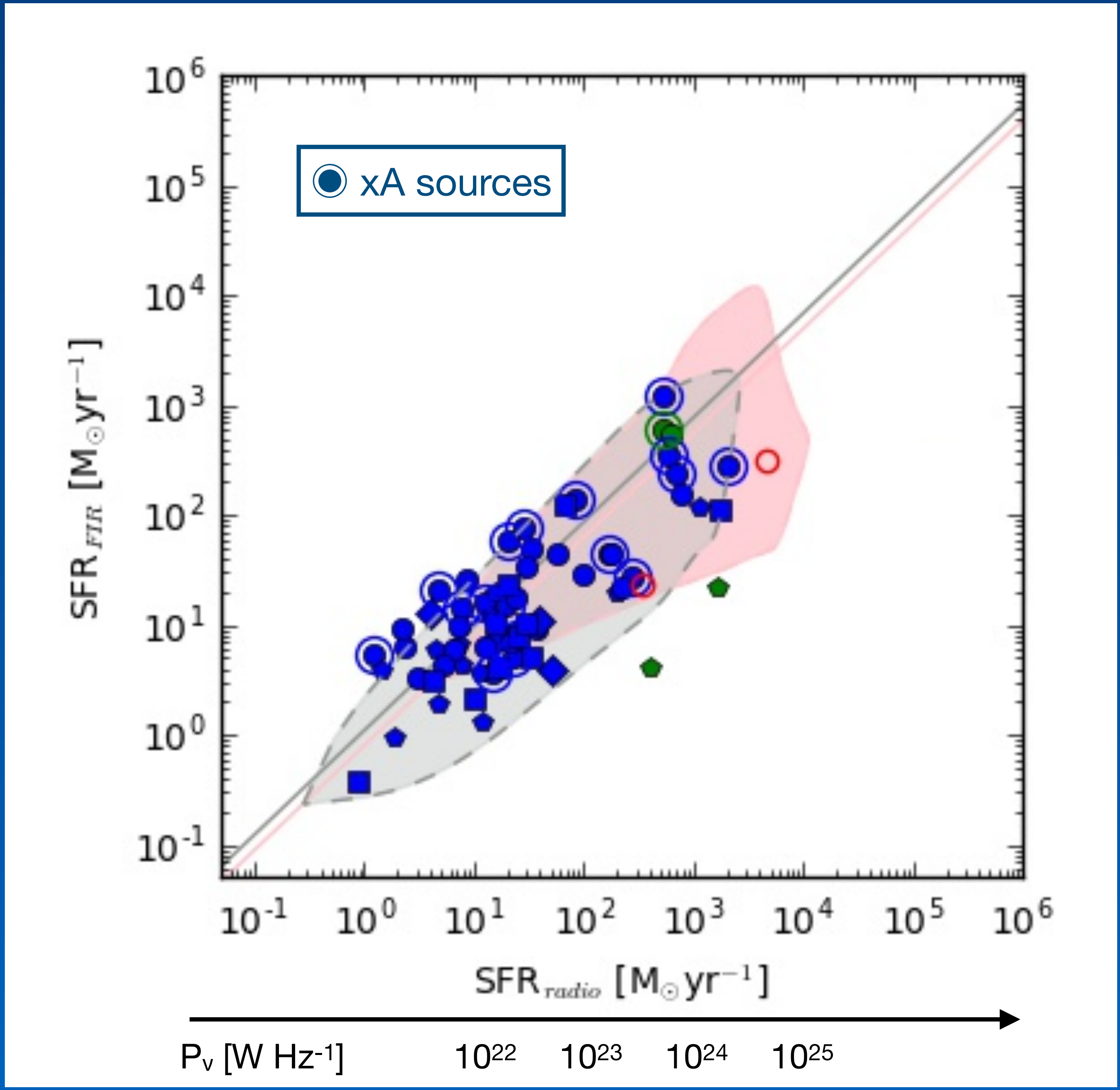

Ganci et al. 2019; del Olmo et al. 2021; cf. Bonzini et al. 2015; talks by Marco Beron and Emilia Järvelä

xA in a particular stage of quasar evolution
Pollution of the line emitting gas by core-collapse supernovae

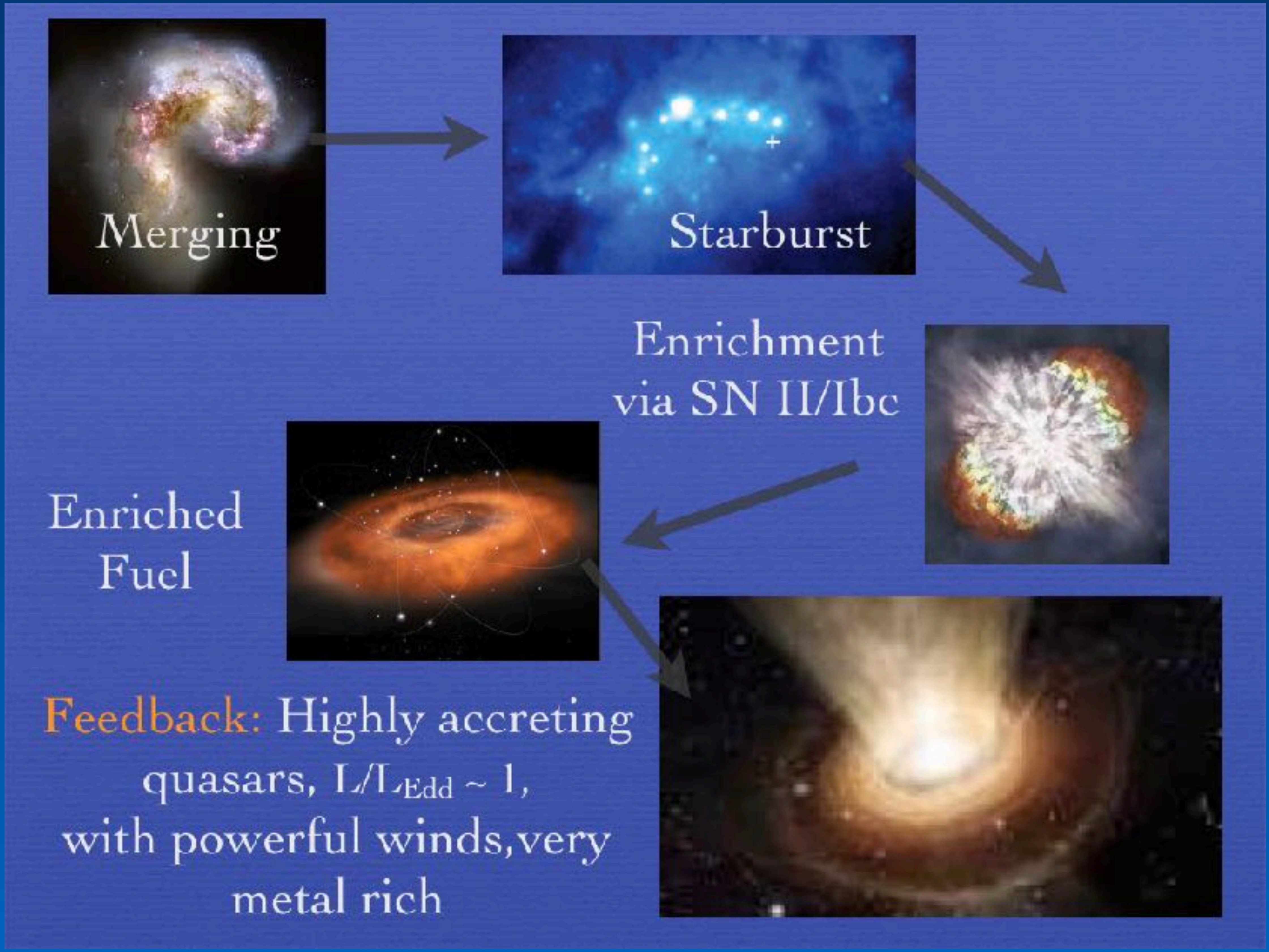

D’Onofrio et al. 2020

The main sequence — Evolutionary interpretation

Cladistic analysis suggests an evolutionary link between Pop. A, B and RL

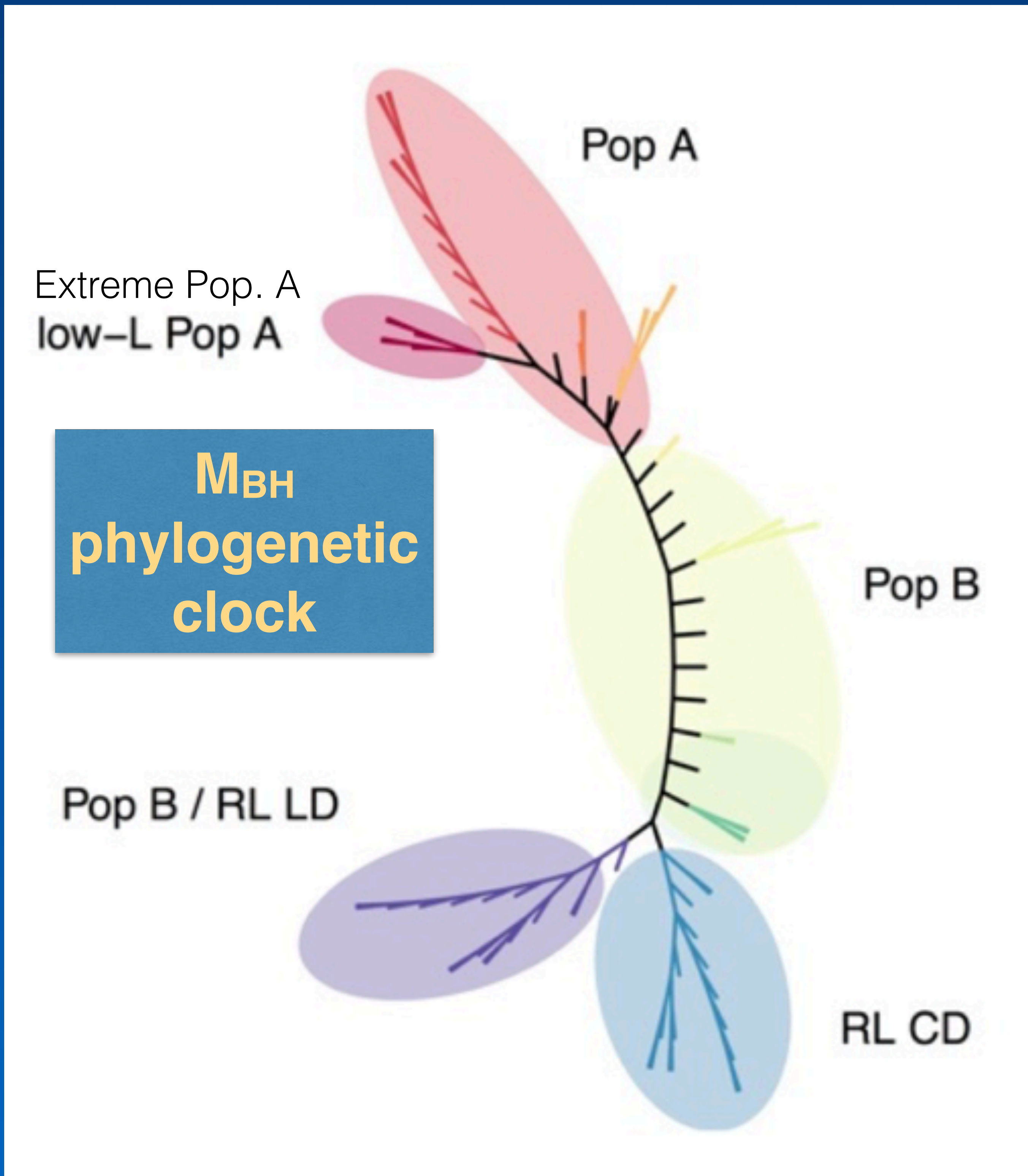

M_{BH} phylogenetic clock

From young / rejuvenated (NLSy1s in extreme Population A, including jetted sources)

Sulentic et al. 2000; Mathur 2000; Komossa et al. 2006; Berton et al. 2017

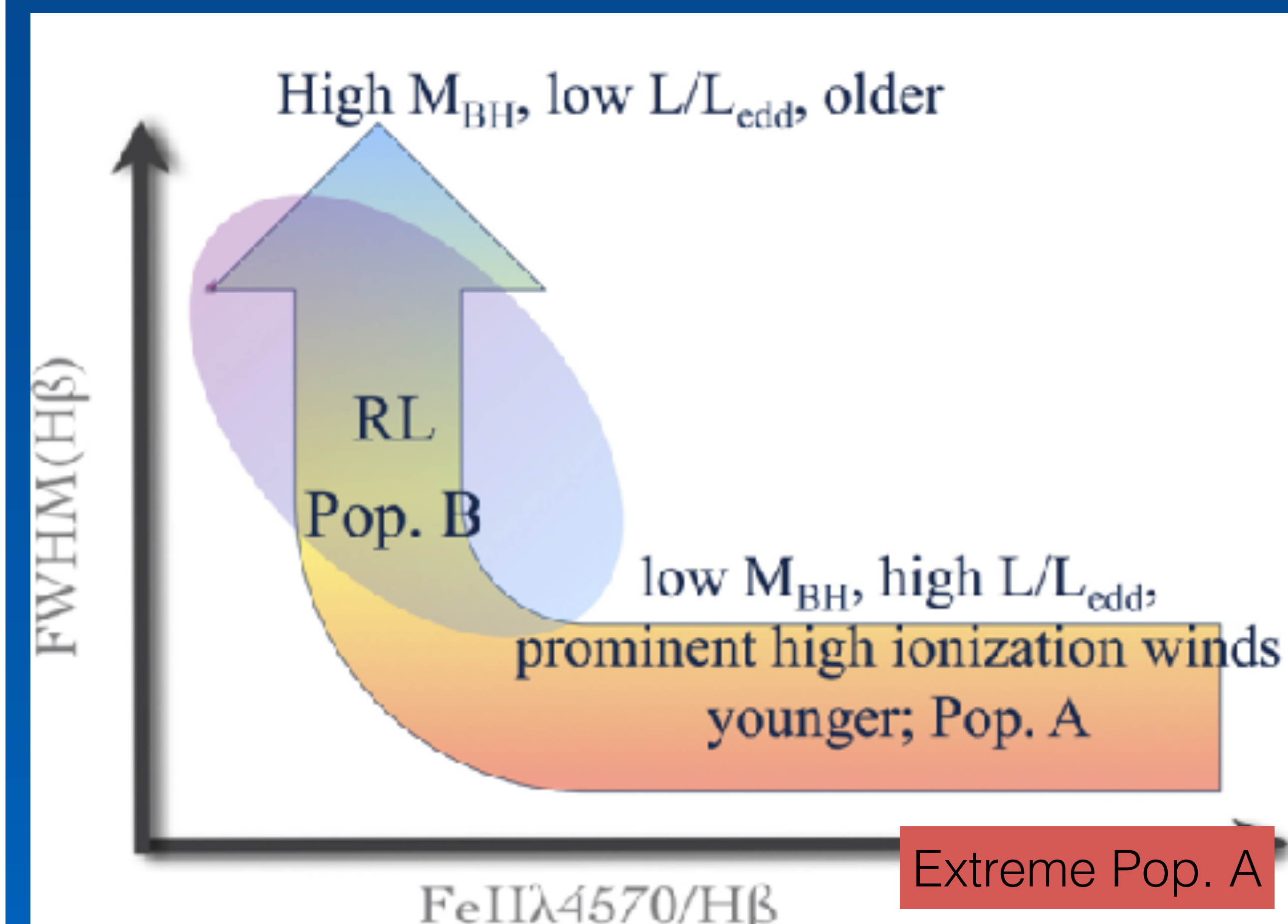

Fraix-Burnet et al. 2017

Applications to Cosmology?

Extreme Population A: “Eddington standard candles”?

xA quasars: Extreme L/L_{Edd} along the MS with small dispersion

Accretion disk theory: low radiative efficiency at high accretion rate; **L/L_{Edd} saturates toward a limiting value**

$$L = \eta L_{\rm Edd} = {\rm const}\, \eta M_{\rm BH}$$

$$L/L_{\rm Edd} \rightarrow {\rm const.} \quad {\rm for} \quad \dot{m} \gg 1$$

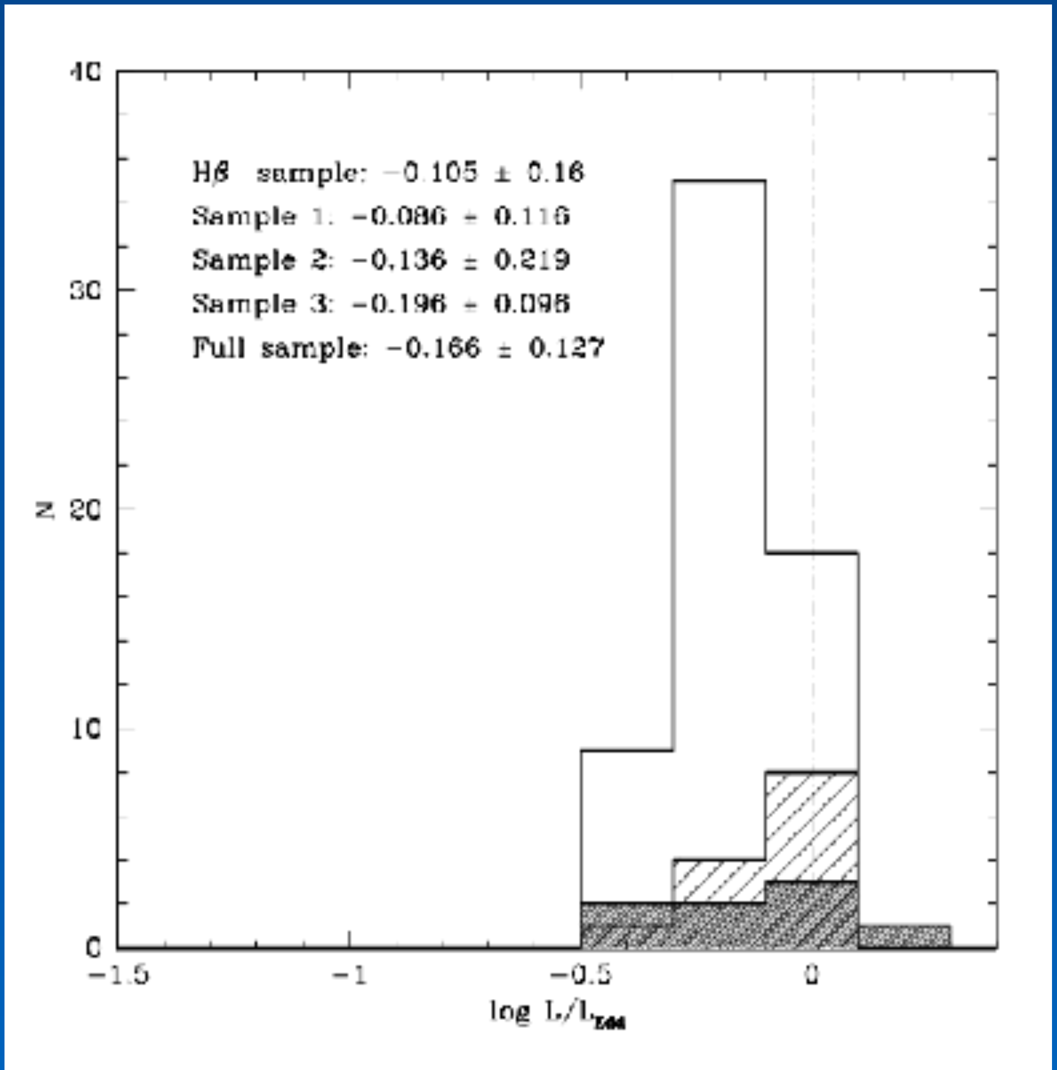

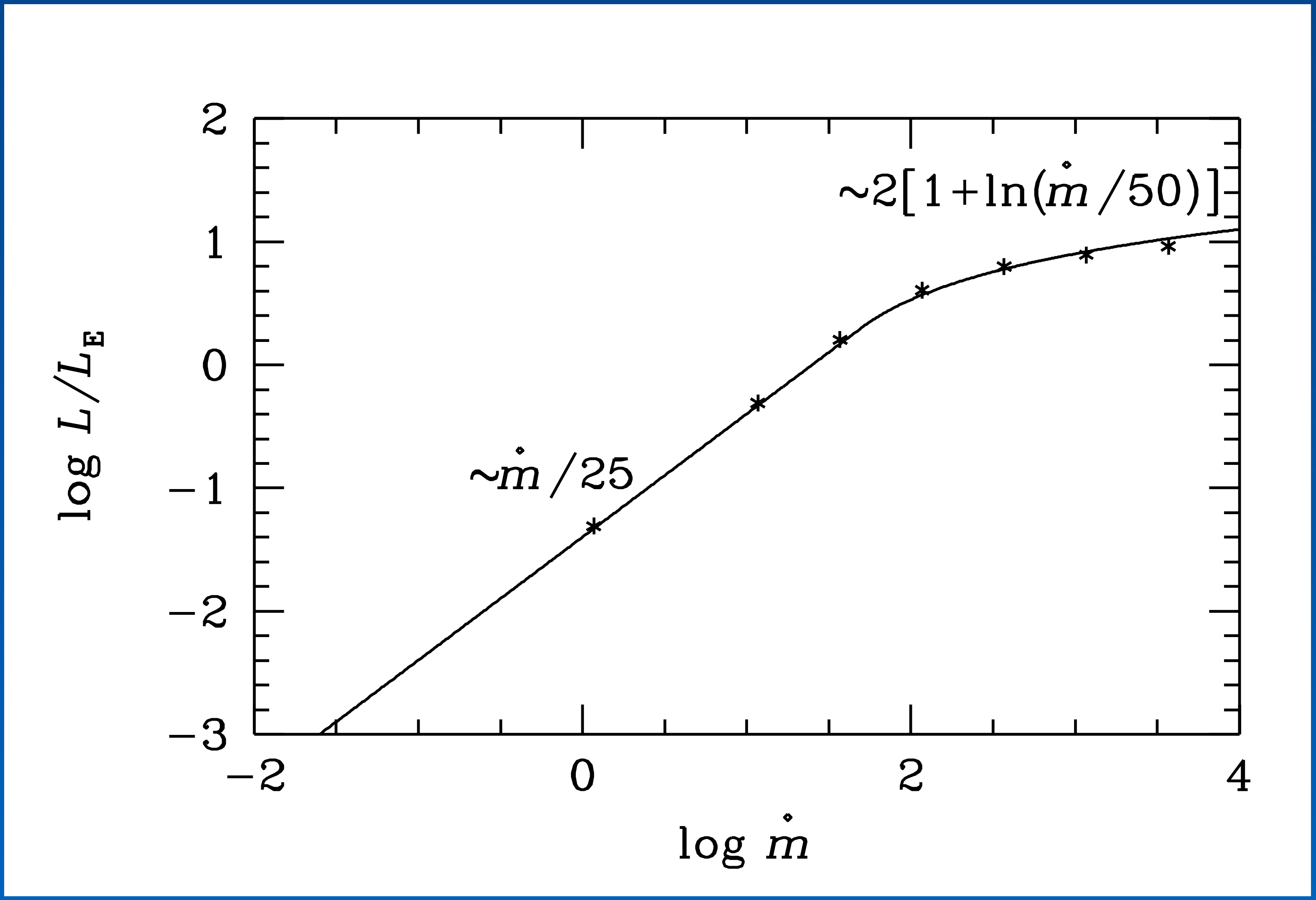

Marziani & Sulentic 2014 (MS14); Mineshige 2000; Abramowicz et al. 1988; Sadowski 2014

Extreme Population A: cosmological applications?

Eddington standard candles

$$M_{BH} = \frac{f r_{BLR} (\delta v)^2}{G}$$

1. **virial motions** of the low-ion. BLR

$$r_{BLR} \propto (\frac{L}{n_{\rm H} U})^{\frac{1}{2}} \propto L^{\frac{1}{2}}$$

2. xA quasars have similar BLR physical parameters (n_H and U), implying that the BLR radius rigorously scales with L as $\mathbf{r_{BLR} \propto (L)^{1/2}}$

$$L = \eta L_{\rm Edd} = {\rm const} \eta M_{\rm BH}$$

1. **xA quasars radiate close to Eddington limit** $\eta \sim 1$

$$L \propto \eta^2 (\delta v)^4 \propto {\rm FWHM}^4$$

4. If we know a **virial broadening estimator δv** (in practice, the FWHM of a low-ionization line), we can derive a *z*-independent luminosity

Analogous to the Tully-Fisher and the early formulation of the Faber Jackson laws for early-type galaxies; and FWHM increases as $L^{1/4}$

Marziani & Sulentic 2014; cf. Teerikorpi 2011

Extreme Population A: "Eddington standard candles"?

A Hubble Diagram for quasars: consistent with concordance ΛCDM

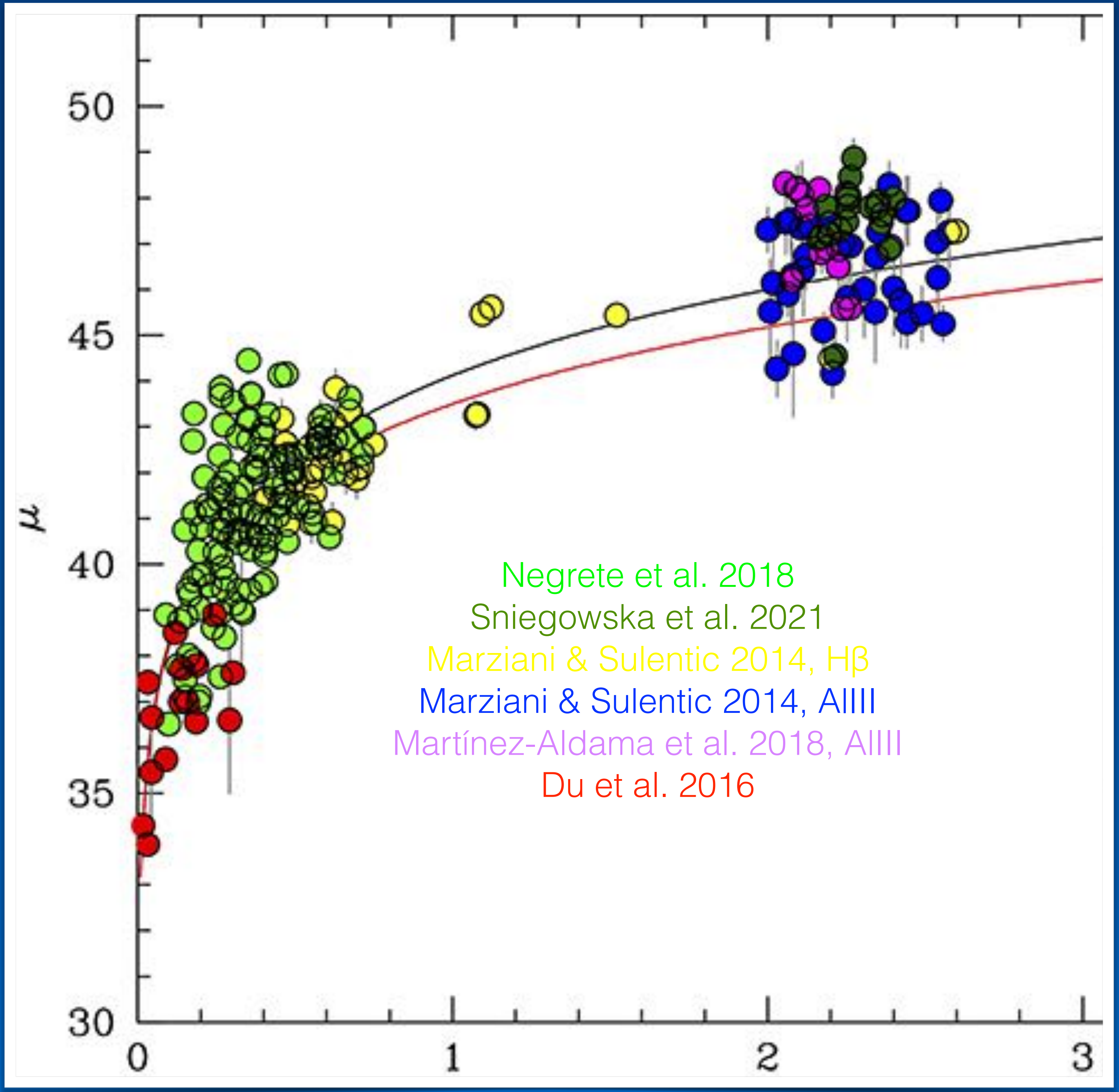

Data already rule out extreme Universes (Ω_Λ=1,Ω_M=0) or the Einstein-de Sitter Universe

Data already provide significant constraints on Ω_M (0.30±0.06), better than supernovae alone, because of the z>1 coverage

Significant scatter, $\sigma_{\Delta\mu}$ ~ 1.1 - 1.3 mag, can be entirely explained by due to viewing angle

Dultzin et al 2020; Czerny et al. 2021

Conclusions

- ❊ interpretation of the quasar main sequence based on Eddington ratio (ratio of radiative to gravitational forces) and orientation

- ❊ Virialized low-ionization and high-ionisation outflow components in the emission lines

- ❊ The MS is not only about spectral parameters; instead, it reflects different evolutionary and environmental situations

- ❊ Extreme Population A: very metal rich, possible enrichment associated with a circumnuclear Starburst

- ❊ Can extreme Population A quasars be exploited as “Eddington standard candles?”

Quasars as distance indicators for cosmology

Sources	Parameters	Basic equation	Reference	Virial
extremely accreting quasars (xA)	Hard X-ray slope, velocity dispersion	$\mathcal{D}_\bullet = \frac{1}{\sqrt{4\pi}}\left[\frac{\ell_0(1+a\ln\dot{m}_{15}) f_{\rm BLR} R_0}{G\kappa_{\rm es}}\right]^{1/2(1-\alpha)} \frac{V_{\rm FWHM}^{1/(1-\alpha)}}{F_{5100}^{1/2}}$	Wang et al.2013	V
extremely accreting quasars (xA)	virial velocity dispersion: FWHM(Hβ) Eddington ratio = const	$L \propto \mathrm{FWHM(H\beta)}^4$	Marziani & Sulentic 2014	V
general quasar populations	X-ray variability, velocity dispersion	$\log\frac{L}{\rm erg\,s^{-1}} + 4\log\frac{\rm FWHM}{10^3\,\rm km\,s^{-1}} = \alpha\log\sigma^2_{\rm rms} + \beta$,	La Franca et al. 2014	V
mainly quasars at z<1	Reverberation mapping time delay τ	$\tau/\sqrt{F} \propto d_L$	Watson et al 2011, 2013; Czerny et al. 2013; Melia 2015	
general quasar populations	non linear relation between soft X and UV	$\log(F_X) = \Phi(F_{UV}, D_L) = \beta' + \gamma\log(F_{UV}) + 2(\gamma-1)\log(D_L)$,	Risalti & Lusso 2016	

Eddington standard candles

Data already rule out extreme Universes (Ω_Λ=1,Ω_M=0) or the Einstein-de Sitter Universe

MS14 data already provided significant constraints on Ω_M ($0.19^{+0.17}_{-0.08}$): the redshift range 2 - 3 is highly sensitive to Ω_M

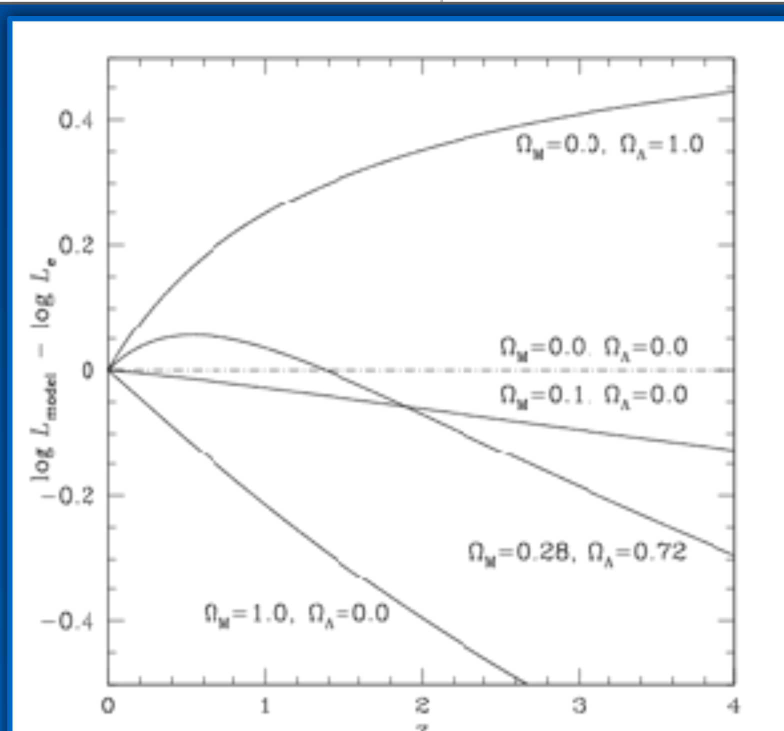

Quasar samples have the potential ability to better constrain Ω_M than supernovae

Samples extending up to z~5 could address the issue of the equation of state of dark energy

Marziani & Sulentic 2014a